CIDER summer school

Partitioning behaviour

Chrystèle Sanloup

Why partitioning matters to relate geophysical and geochemical heterogeneity in the deep Earth?

- F. Albarède, Geochemistry (2009): 'The Earth is a complex body whose dynamics are controlled by mechanisms that commonly work in opposing directions:'
  1) differentiation mechanisms maintained by **fractionation of elements** and isotopes between the phases
  2) mixing mechanisms

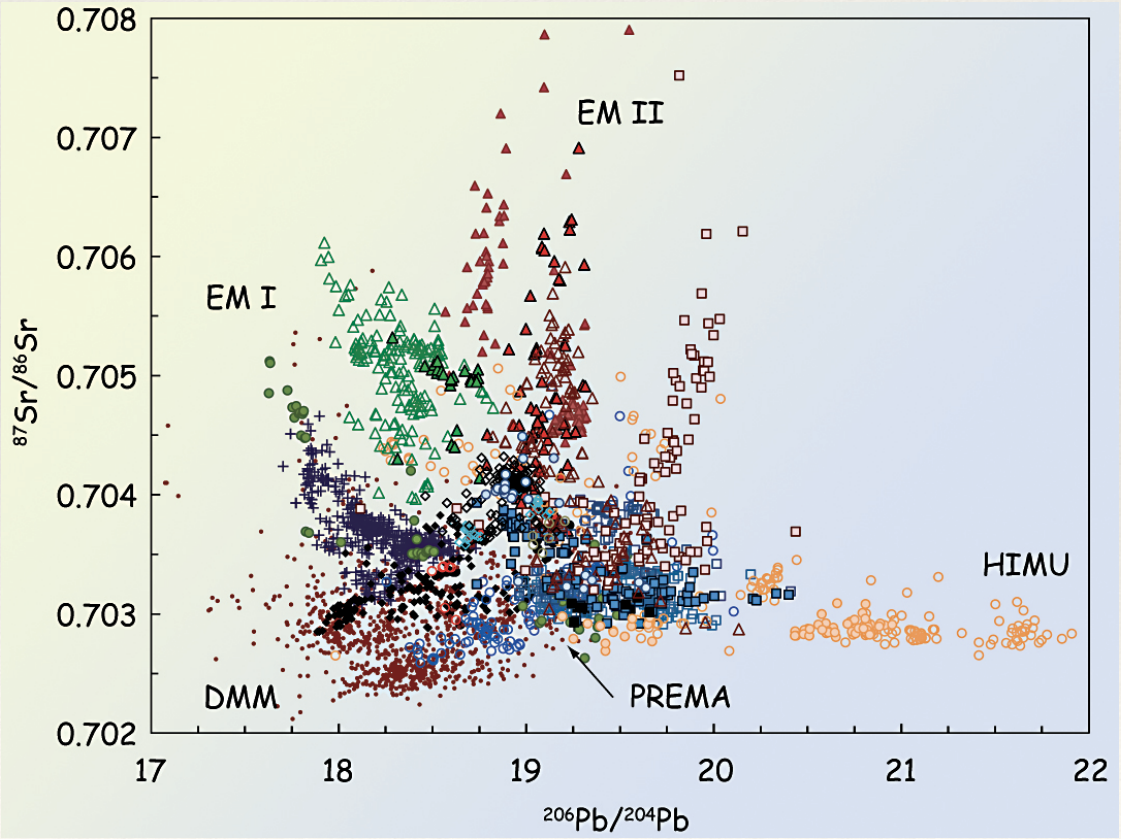

Sr-Pb isotope systematics in oceanic basalts
White Geochem. Persp. 2015

Geochemical heterogeneities: where do they stem from? which can be tested geophysically?

Why partitioning matters to relate geophysical and geochemical heterogeneity in the deep Earth?

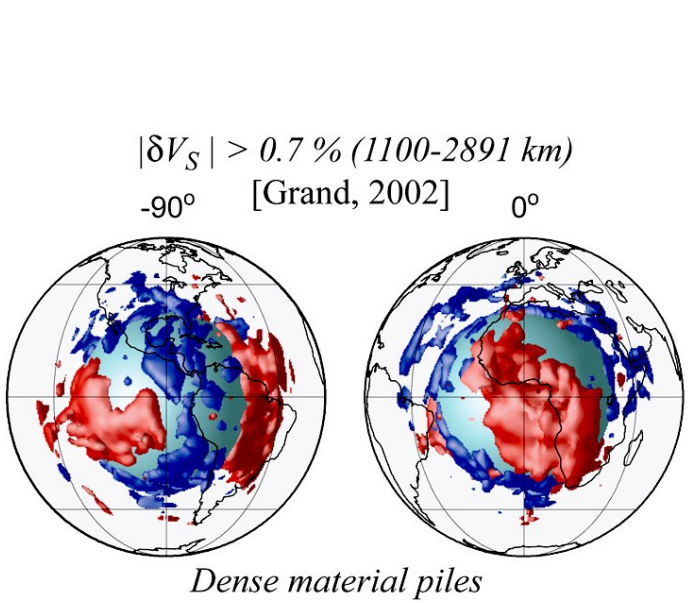

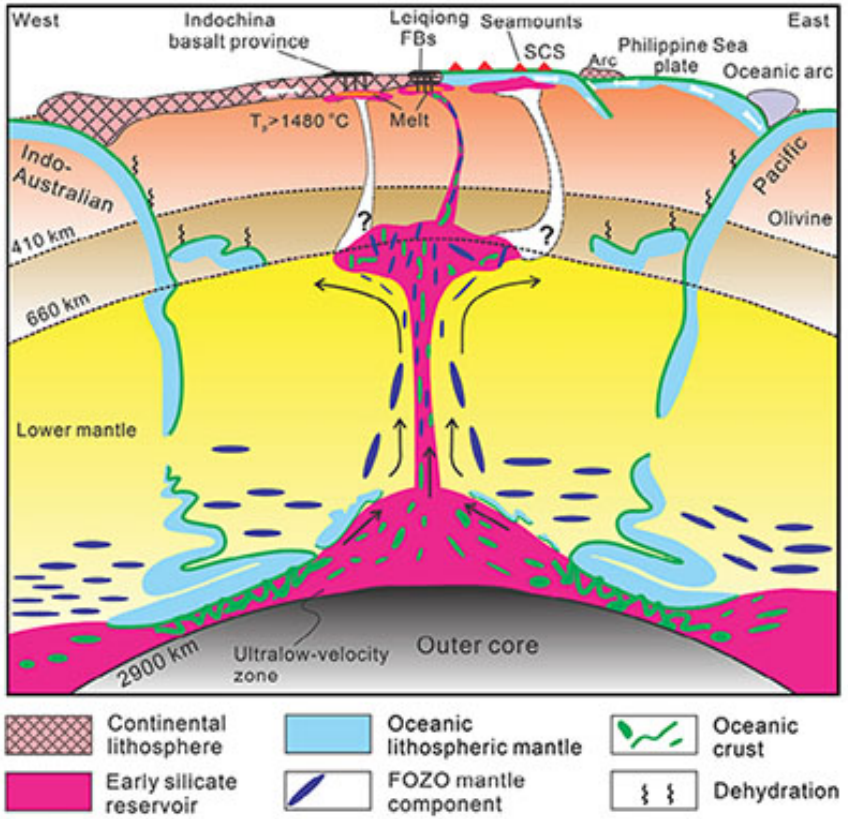

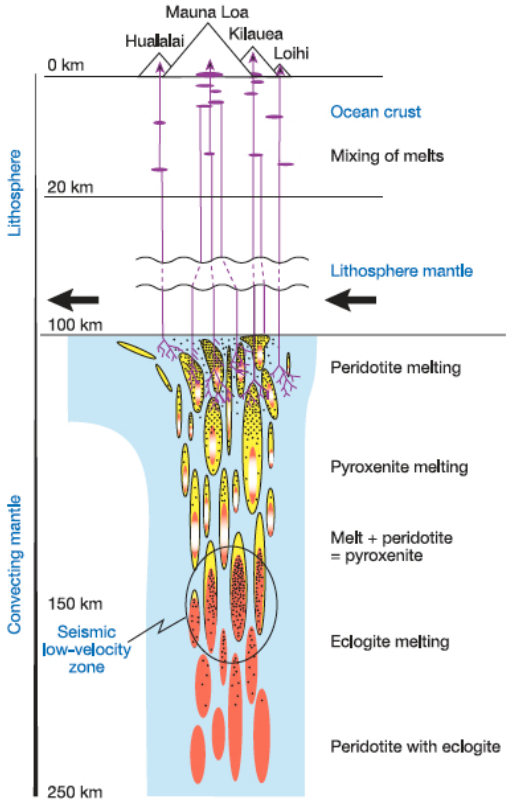

Sobolev Nature 2005

Partitioning of trace elements: to understand heterogeneities at depth

Partitioning of major elements: case of Fe

Outline

partition coefficient: $D^i_{1/2} = \frac{C^i_1}{C^i_2}$

- why it matters?
- how to measure it for trace elements?
- thermodynamics: how to be predictive?
- influence of melt structure
- case of a major element: Fe

What can we learn from measuring partition coefficients?

- petrology: fraction of melt, mineral phases at the residue (spider diagrams), fractional *vs* equilibrium or batch melting

$$\frac{\mathrm{d}C^i_{\mathrm{liq}}}{C^i_{\mathrm{liq}}} = \left(D^i_{\mathrm{s/l}} - 1\right)\frac{\mathrm{d}F}{F} \qquad C^i_{\mathrm{liq}} = \frac{C^i_{\mathrm{source}}}{F + (1-F)\,D^i_{\mathrm{s/l}}}$$

- estimate P, T, fO_2, composition (hence heterogeneity!) of the melting source and more generally of the fractionation process (e.g. crust formation)
- quantify fluxes between reservoirs for geological cycles

Why partitioning matters to relate geophysical and geochemical heterogeneity in the deep Earth?

- dating formation of reservoirs
  W/Hf fractionation in case of planetary core formation

Righter et al. GCA 1993

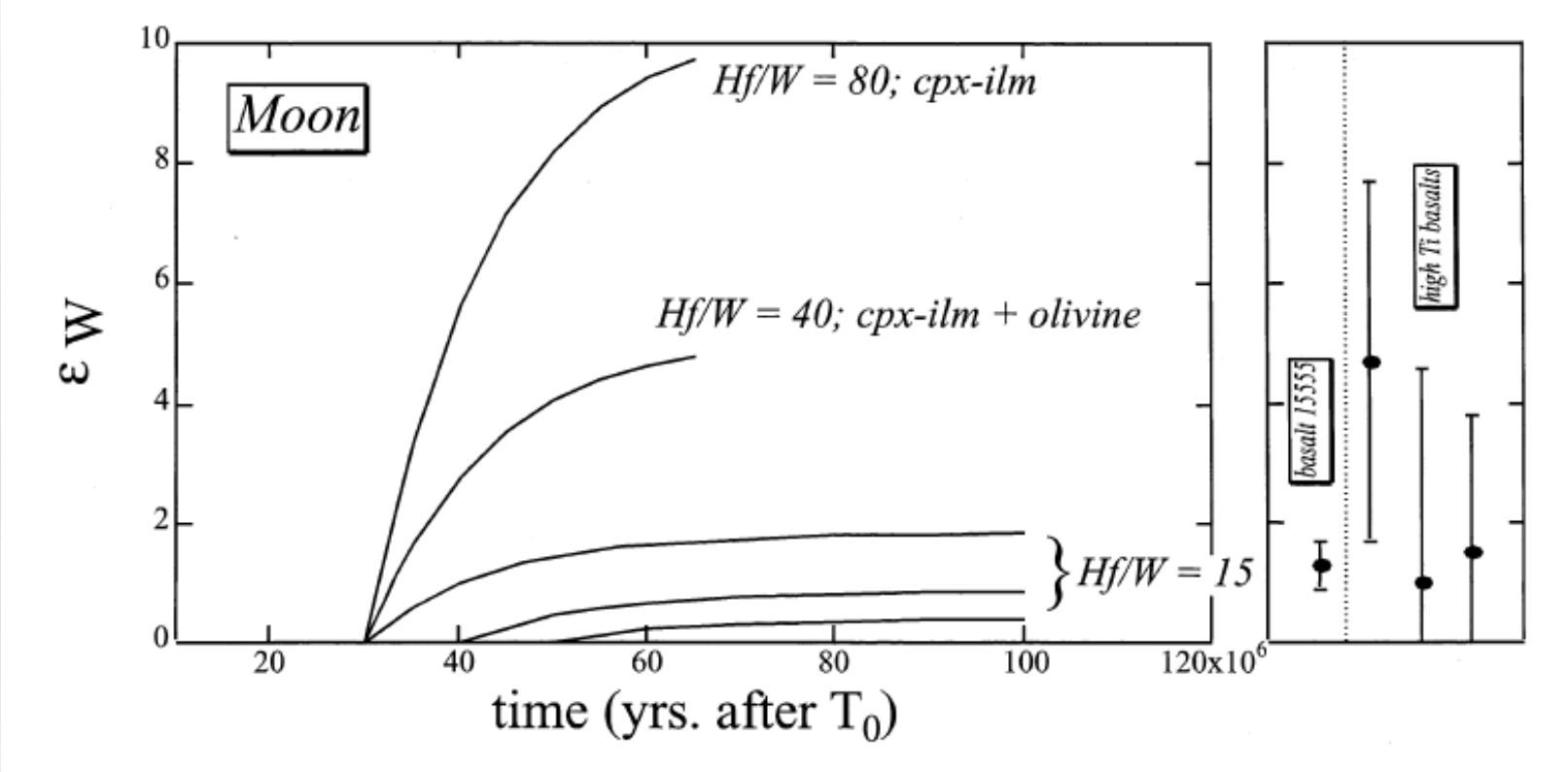

Partitioning and geochemical affinity

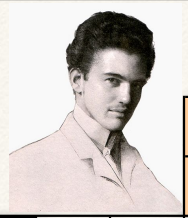

1 H																	2 He
3 Li	4 Be											5 B	6 C	7 N	8 O	9 F	10 Ne
11 Na	12 Mg											13 Al	14 Si	15 P	16 S	17 Cl	18 Ar
19 K	20 Ca	21 Sc	22 Ti	23 V	24 Cr	25 Mn	26 Fe	27 Co	28 Ni	29 Cu	30 Zn	31 Ga	32 Ge	33 As	34 Se	35 Br	36 Kr
37 Rb	38 Sr	39 Y	40 Zr	41 Nb	42 Mo	43 (Tc)	44 Ru	45 Rh	46 Pd	47 Ag	48 Cd	49 In	50 Sn	51 Sb	52 Te	53 I	54 Xe
55 Cs	56 Ba	57 La*	72 Hf	73 Ta	74 W	75 Re	76 Os	77 Ir	78 Pt	79 Au	80 Hg	81 Tl	82 Pb	83 Bi	84 Po	85 At	86 Rn
87 Fr	88 Ra	89 Ac**															

Os *siderophile* Cu *chalcophile* Rb *lithophile* N *atmophile*

Goldschmidt 1937

- Goldschmidt (1929): elements partitioned within 4 shells in the molten early Earth: atmosphere, silicate, Fe-S and Fe, hence the 4 affinities.
- siderophile
- atmophile/volatile
- compatible/incompatible
- Godlschmidt (1937) understood the principal controls on substitution are the mismatch in valence and ionic radius between the substituent and substituted ion

$^{182}Hf/^{182}W$

$^{129}I/^{129}Xe$

$^{146}Sm/^{142}Nd$

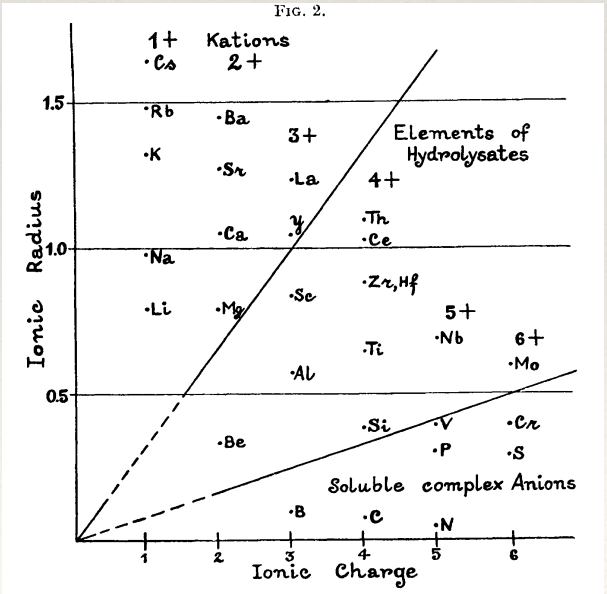

Partitioning experiments

Beattie Chem. Geol. 1994

- some definitions:

partition coefficient: $D^i_{1/2} = \frac{C^i_1}{C^i_2}$ Bulk partition coefficient: $D^i_{s/l} = \Sigma_j \frac{x_j C^i_{s_j}}{C^i_l}$

exchange partition coefficient: $K^{M/N}_{1/2} = \frac{\frac{C^M_1}{C^M_2}}{\frac{C^N_1}{C^N_2}}$

- trace elements: very low abundances
- electron microprobe analyses: down to 100 ppm for REE
- LA-ICPMS measurements : down to ppb-ppt level
- SIMS: Ion microprobe analyses; and nanoSIMS for small samples

Crystal/melt partitioning experiments

- case of tungsten at ambient P
- LA-ICPMS measurements
- Need of standards

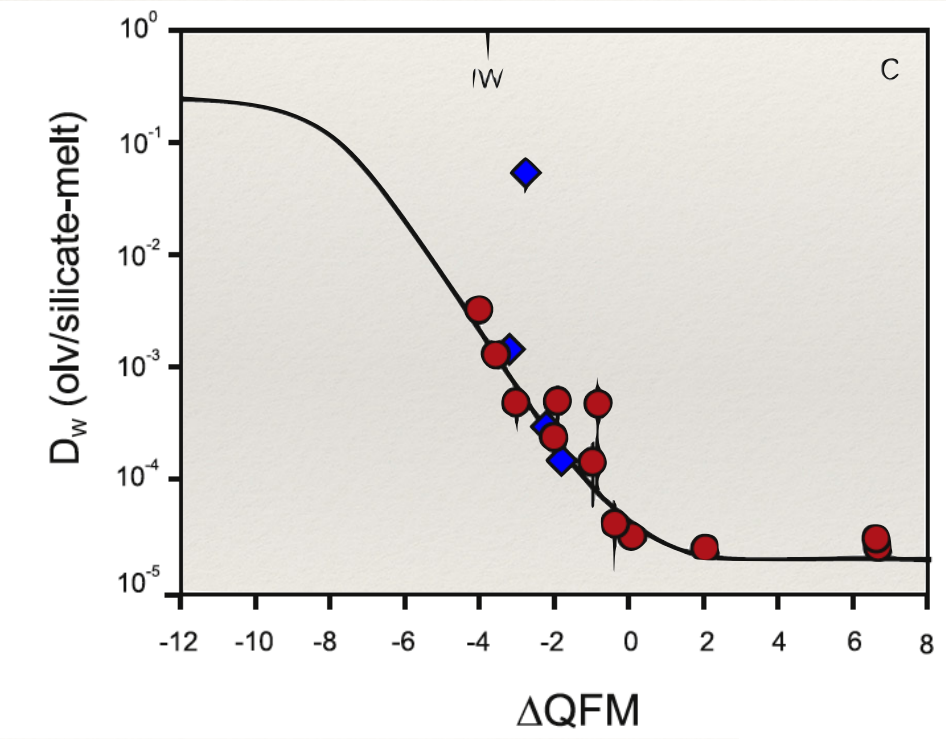

Fonseca et al. EPSL 2014

Leitzke et al. EPSL 2017

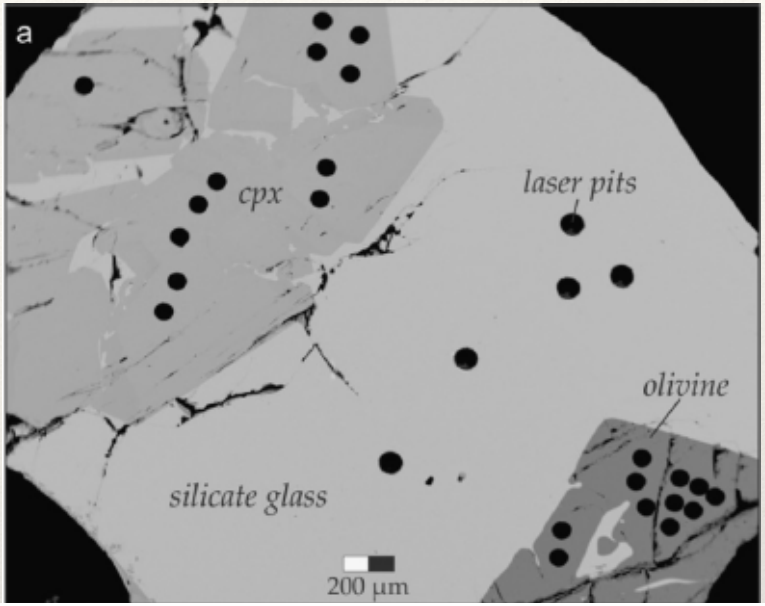

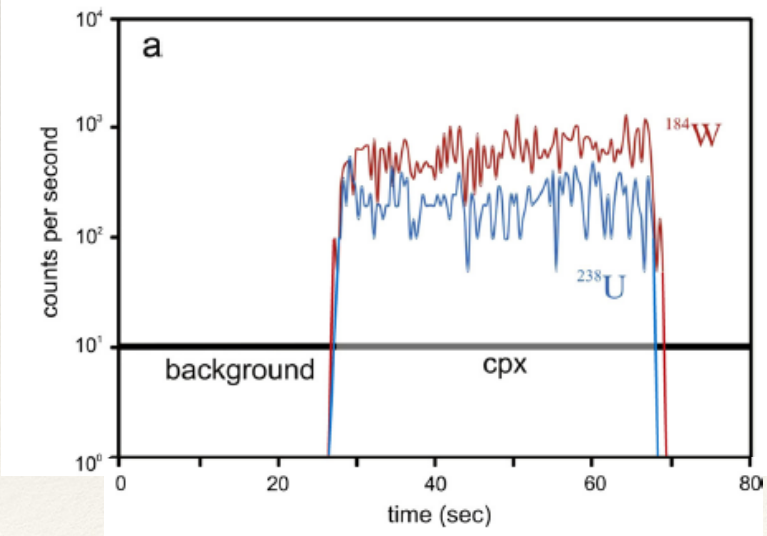

Crystal/melt partitioning experiments

- trace elements: very low experimental abundances may still be higher than natural abundances
- Henry's law violated if partitioning mechanism changes with concentration
- not the case for REE, but can happen for siderophile elements

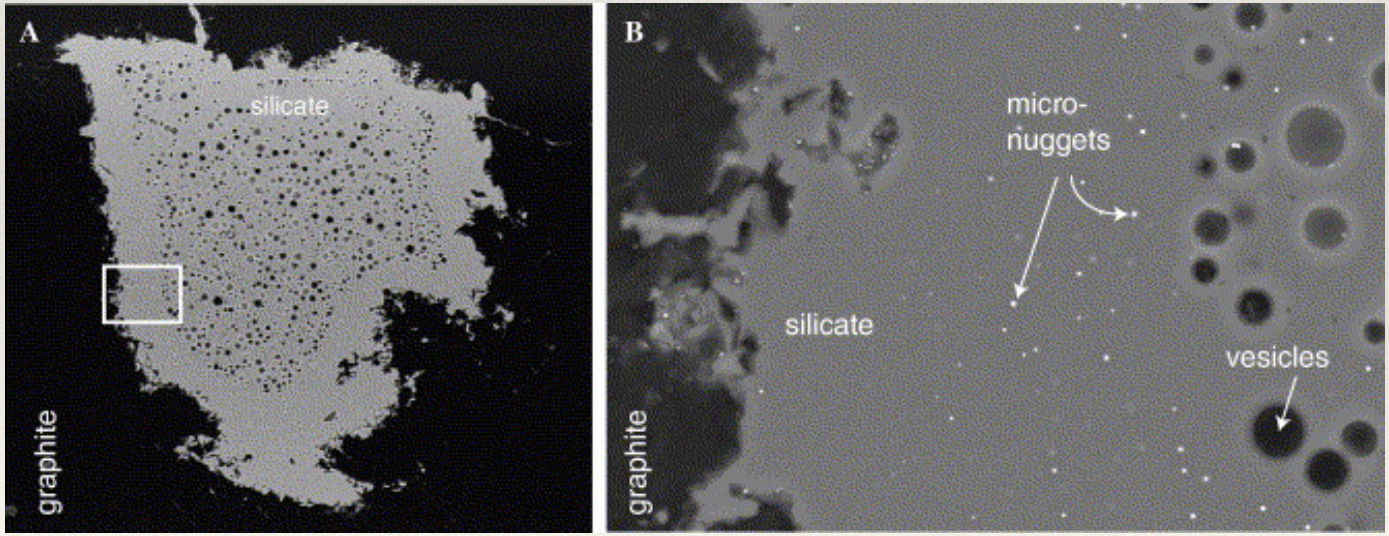

Cottrell and Walker GCA 2006

Partitioning in the upper mantle

- Garnet: "host of incompatible trace elements"
- Most studies conducted up to 3.5 GPa

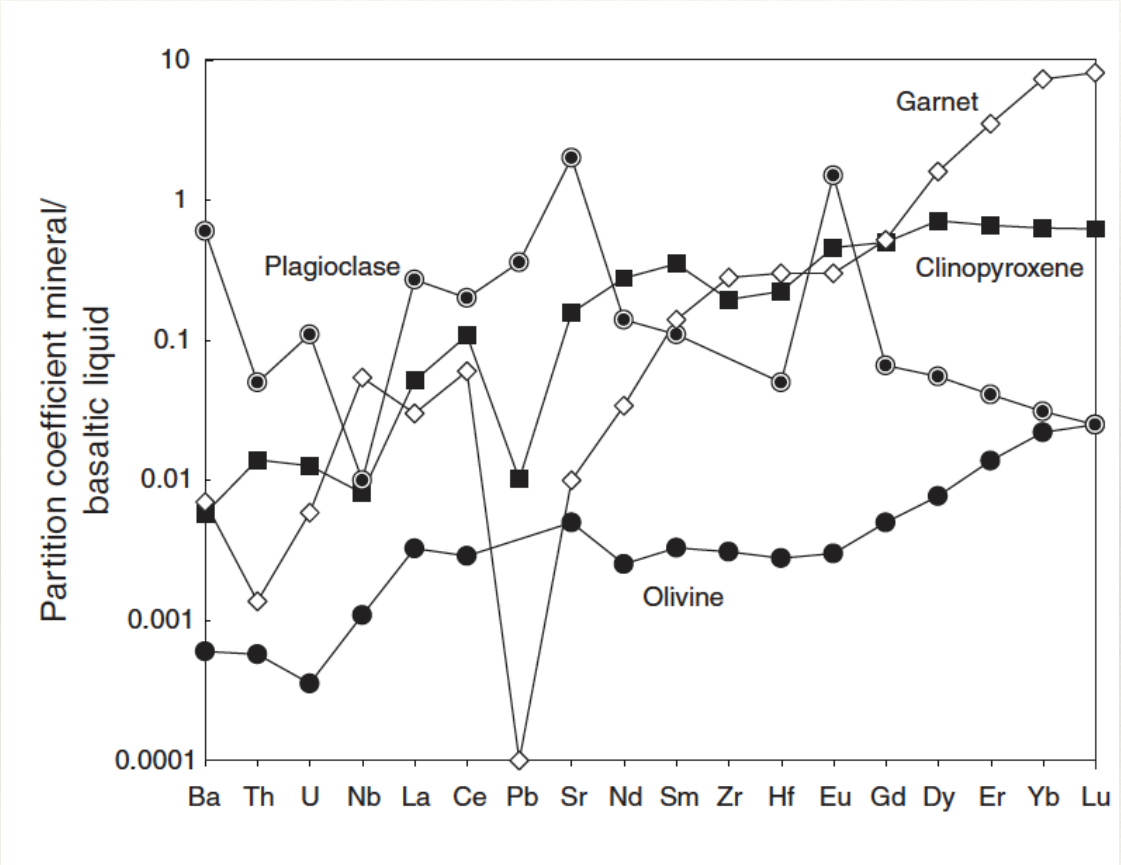

Typical mineral/basalt partition coefficients
Albarede Geochemistry 2009

Partitioning in the mantle

Mineral proportion in MORB at depth

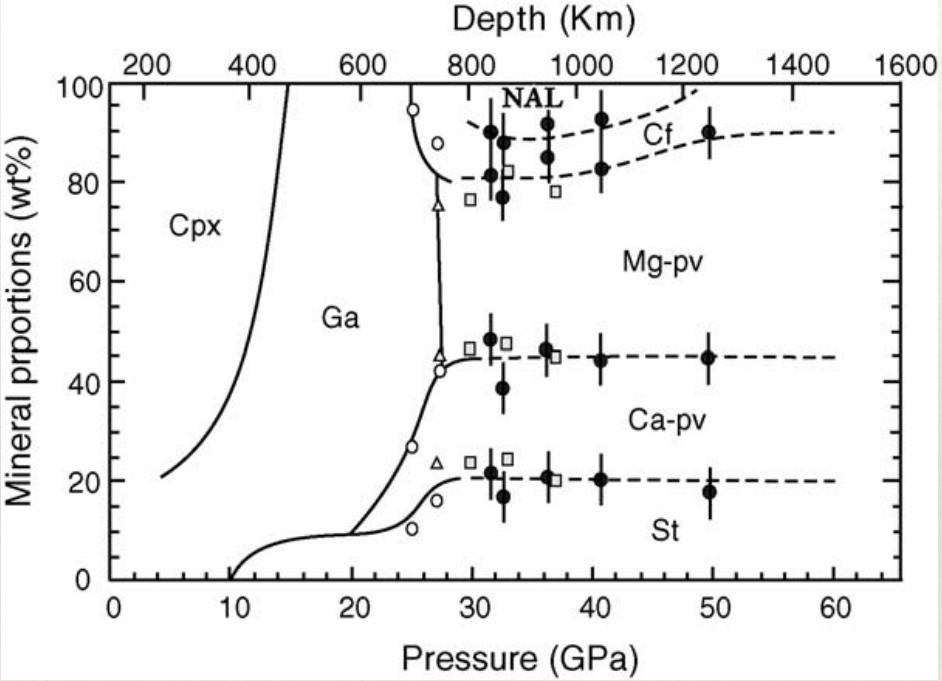

Perrillat et al. JGR 2006

Majorite/melt

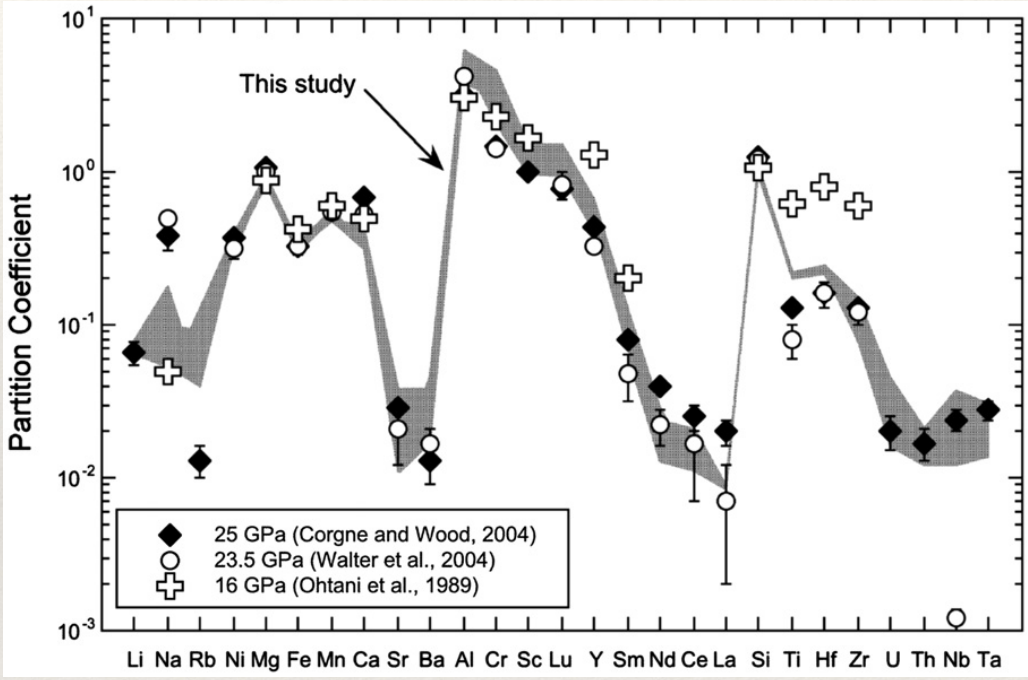

Corgne et al. Lithos 2012

Partitioning in the lower mantle

- Ca-bridgmanite: "garnet of the lower mantle"

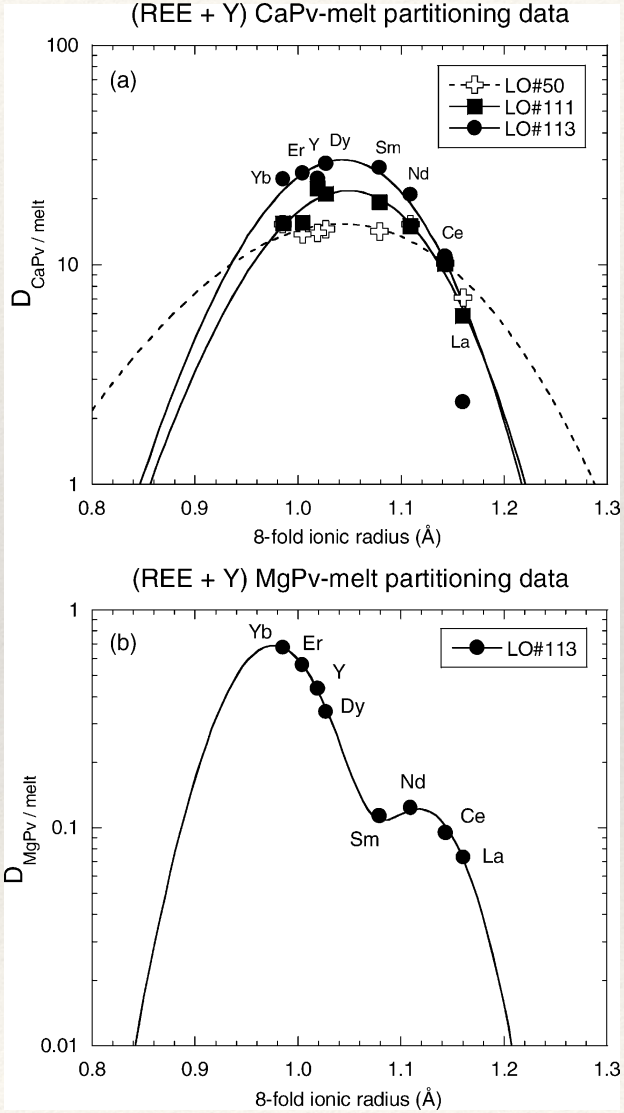

Hirose et al. PEPI 2004

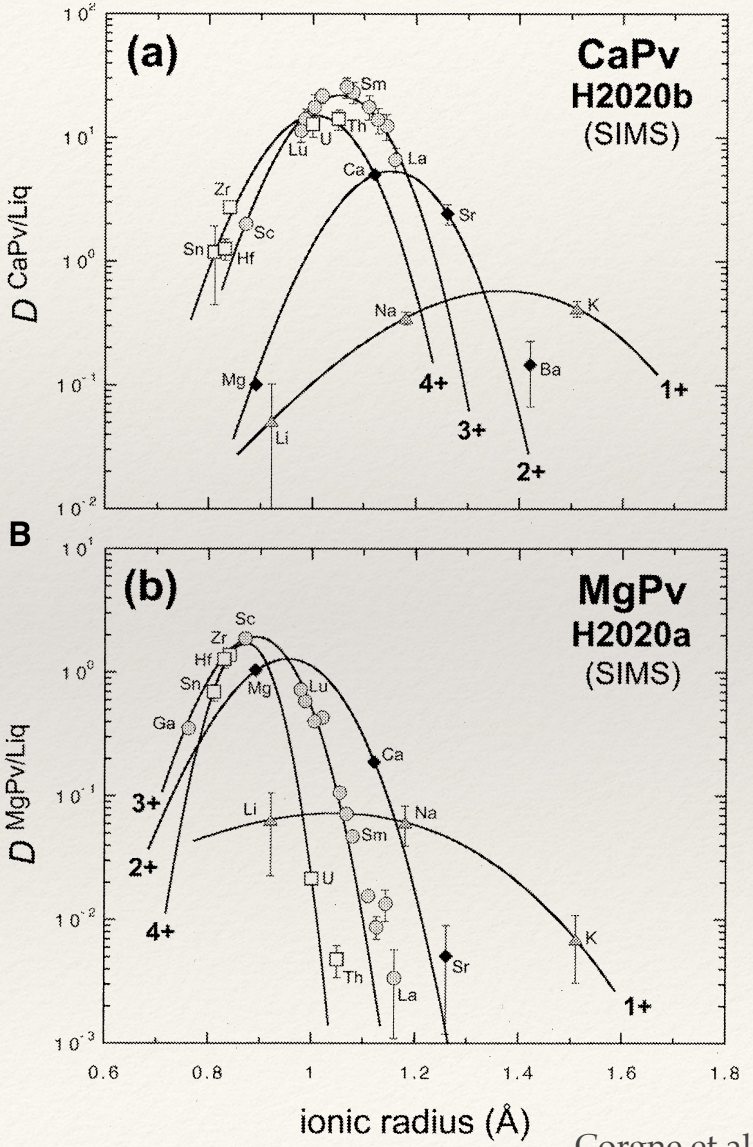

Corgne et al. GCA 2005

Partitioning in the lower mantle

- Record: up to 135 GPa in laser-heating diamond-anvil cells Tateno et al. 2018.

- SEM image of recovered sample (69 GPa) after LA-ICPMS analyses

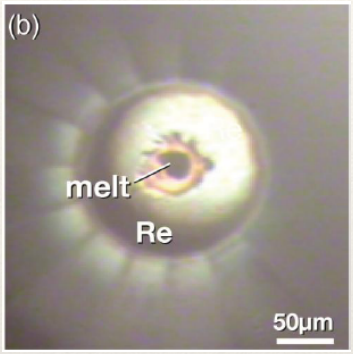

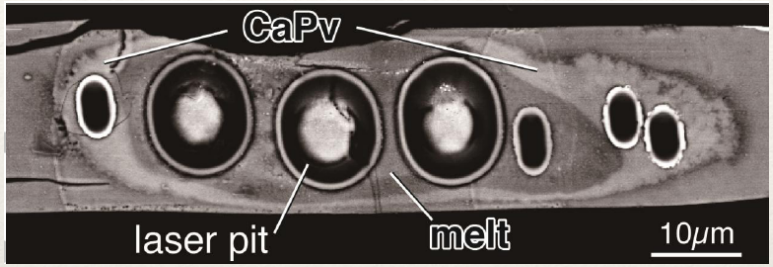

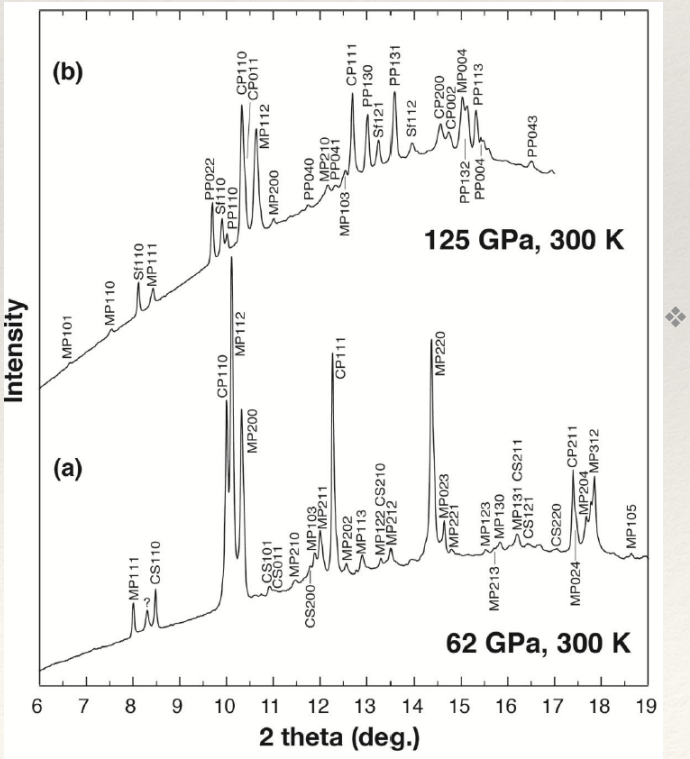

- In situ X-rays
  => mineralogy / crystallography known

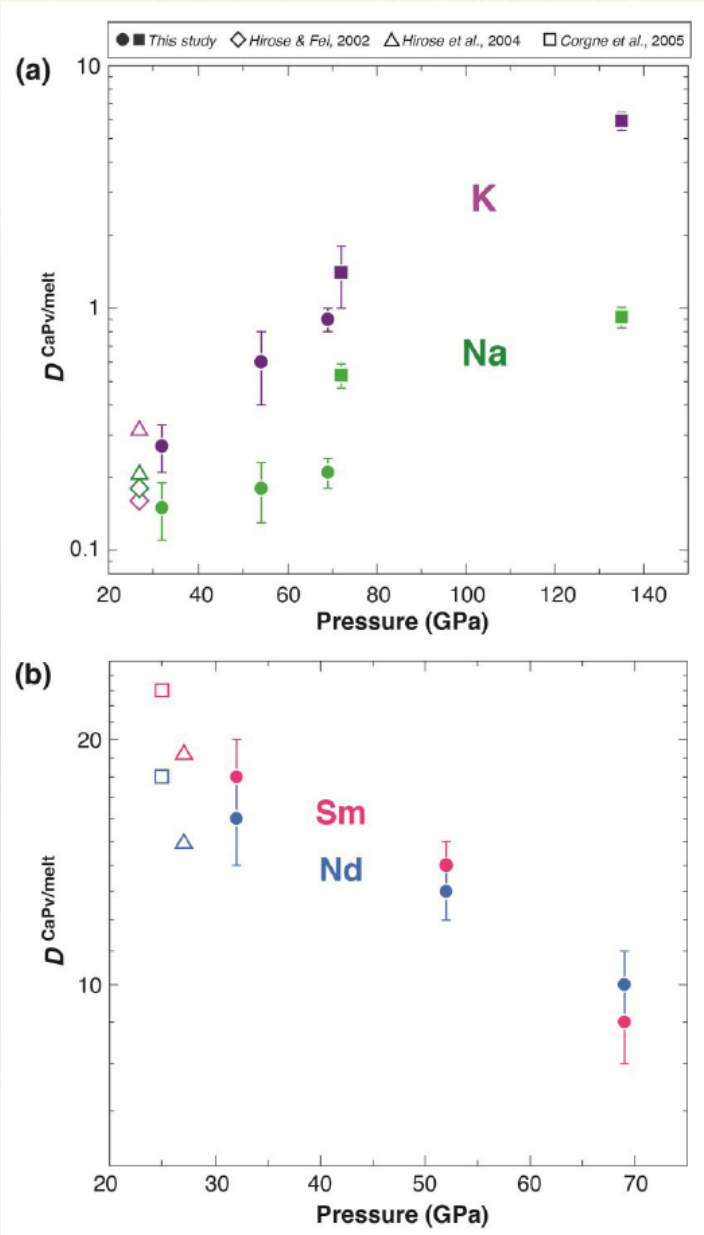

Pushing the limits

- DAC experiments and nanoSIMS
- shock experiments
- X-ray fluorescence

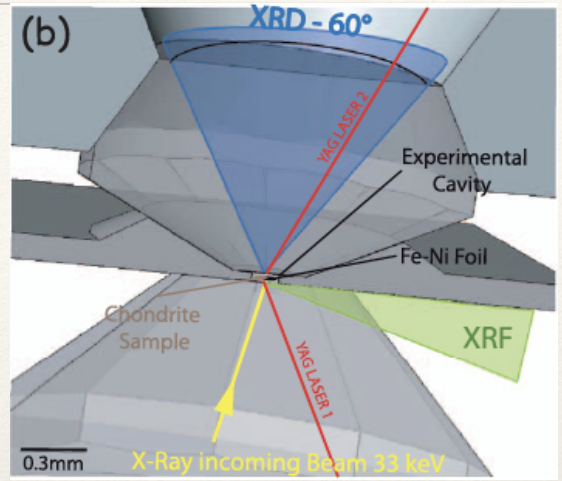

- case of fluid/melt partitioning (fluid can't be quenched)
- case of elements that move upon quenching: volatiles/gases
- in situ mapping possible

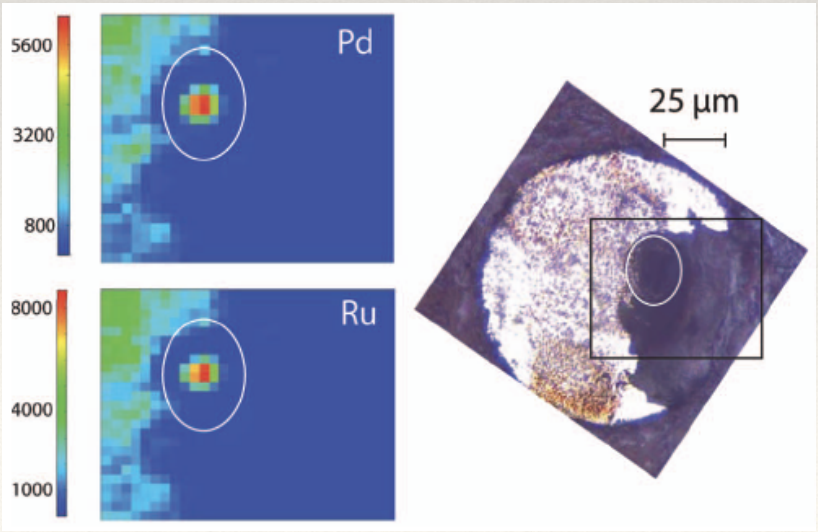

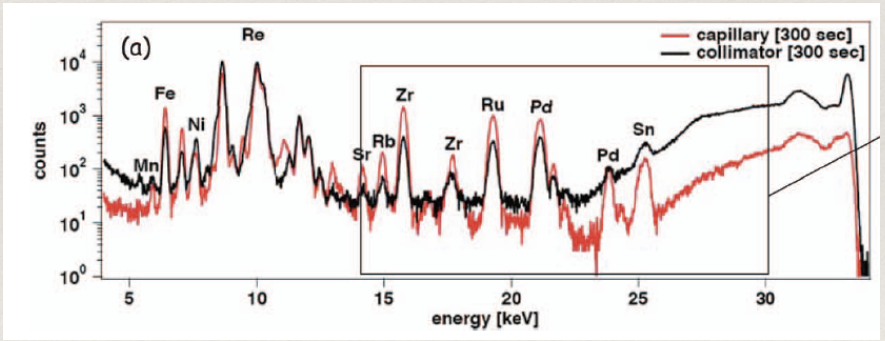

X-ray fluorescence data collected at 50 GPa on chondrite sample

Petitgirard et al. Rev. Sci. Instrum. 2012

Thermodynamics

Substitution of element M^{2+} for Mg in olivine: $MO_{liq} + Mg_2SiO_4 \rightleftharpoons MgO_{liq} + MMgSiO_4$

Beattie Chem. Geol. 1994

At equilibrium: $\Delta G = 0$

1) $G = H - TS$

$= U + PV - TS$

$\Rightarrow dG = \delta Q + \delta W + PdV + VdP - TdS - SdT$

$= -SdT + VdP$

$\Rightarrow \left(\frac{\partial G}{\partial T}\right)_P = -S$ and $\left(\frac{\partial G}{\partial P}\right)_T = V$

2) For an ideal gas: $\left(\frac{\partial G}{\partial P}\right)_T = V$ and $PV = nRT \Rightarrow G(P,T) = G_0(T) + nRT \ln \frac{P}{P_0}$

G is an extensive property, *i.e.* for i components:
(number of moles n_i)

$$G(P,T) = \sum_i n_i \left(\mu_0^i(T) + RT \ln \frac{P_i}{P_0}\right)$$

$$= \sum_i n_i \mu_i$$

μ_i: chemical potential

3) For a mixture of real gases:

$$G(P,T) = \sum_i n_i \left(\mu_0^i(T) + RT \ln \frac{f_i}{P_0}\right)$$

f_i : gas fugacity

For a mixture of condensed phases:

$$G(P,T) = \sum_i n_i \left(\mu_0^i(T,P) + RT \ln a_i\right)$$

a_i : activity

Thermodynamics

Substitution of element M^{2+} for Mg in olivine: $MO_{liq} + Mg_2SiO_4 \rightleftharpoons MgO_{liq} + MMgSiO_4$

At equilibrium: $\Delta G = 0$ Beattie Chem. Geol. 1994

$$\Delta G(P,T) = \Delta G_0(P,T) + RT\left(\ln a_{MgO} + \ln a_{MMgSiO_4} - \ln a_{MO} - \ln a_{Mg_2SiO_4}\right)$$

$$= \Delta G_0(P,T) + RT\left(\ln \frac{a_{MgO}a_{MMgSiO_4}}{a_{MO}a_{Mg_2SiO_4}}\right) = \Delta G_0(P,T) + RT\ln K$$

Assumption: non-ideality, $\gamma = \frac{a}{x}$,for element M is the same in both olivine and melt

$$\Delta G = \Delta G_0 + RT\left(\ln \frac{x_{MgO}x_{MMgSiO_4}}{x_{MO}x_{Mg_2SiO_4}}\right) \qquad \Rightarrow D_M^{ol/melt} = D_{Mg}^{ol/melt}\exp\left(-\frac{\Delta G_0}{RT}\right)$$

More generally: $$\frac{x_i^{phase1}}{x_i^{phase2}} = D(T,P,composition,fO_2) = k_0\exp\left(-\frac{\Delta G_0}{RT}\right)$$

Thermodynamics

Substitution of element M^{2+} for Mg in olivine: $MO_{liq} + Mg_2SiO_4 \rightleftharpoons MgO_{liq} + MMgSiO_4$

$$\frac{x_M^{olivine}}{x_M^{melt}} = D_M^{olivine/melt}(T,P) = D_{Mg} \exp\left(-\frac{\Delta G_0}{RT}\right)$$

to have quantitative predictions of partitioning as a function of P, T:

$$\ln D_M(T,P) = \ln D_{Mg} - \left(\frac{\Delta H_0(T) - T\Delta S_0(T) + P\Delta V_0(T)}{RT}\right)$$
$$= a + \frac{b}{T} + \frac{cP}{T}$$

=> multi-regression analysis to data as a function of T and P

$$\ln D(T,P,composition,fO_2) = a + \frac{b}{T} + \frac{cP}{T} + dfO_2 + e(nbo/t)$$

Crystal/melt partitioning experiments

- effect of fO_2 on partitioning:
  Metal/silicate partitioning of element W^{4+} or W^{6+}: $W_{metal} + x/4 O_2 \rightleftharpoons W^{x+}O_{x/2}$

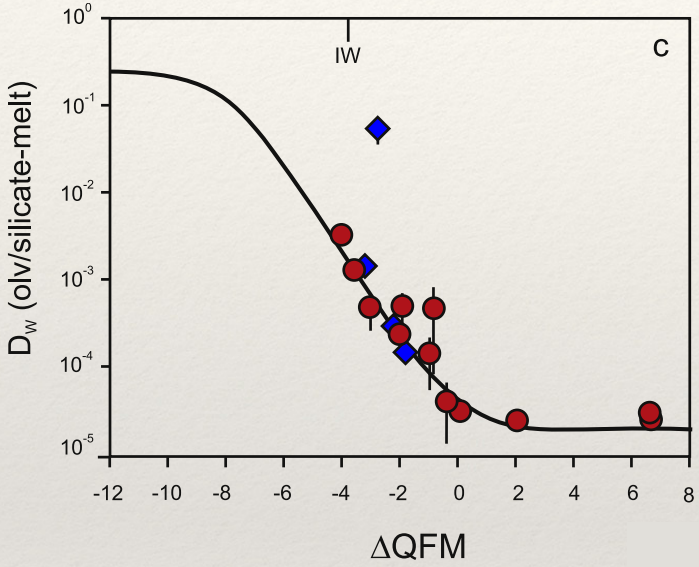

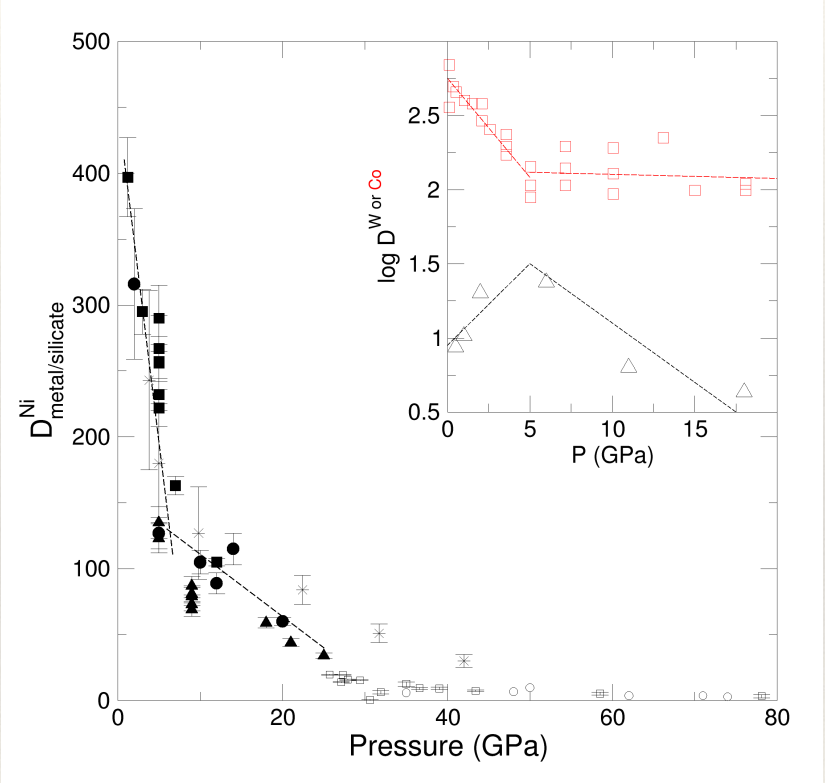

$$D_M^{crystal/melt} = \frac{D_{M^{4+}}^{crystal/melt} K (fO_2)^{-1/2} + D_{M^{6+}}^{crystal/melt}}{1 + K (fO_2)^{-1/2}}$$

Fonseca et al. EPSL 2014, Mallmann and O'Neill 2007 & 2009

W data: Cottrell et al. EPSL 2009

Crystal/melt partitioning experiments

- effect of fO_2 on partitioning, input from EXAFS

Wade et al. Chem. Geol. 2013

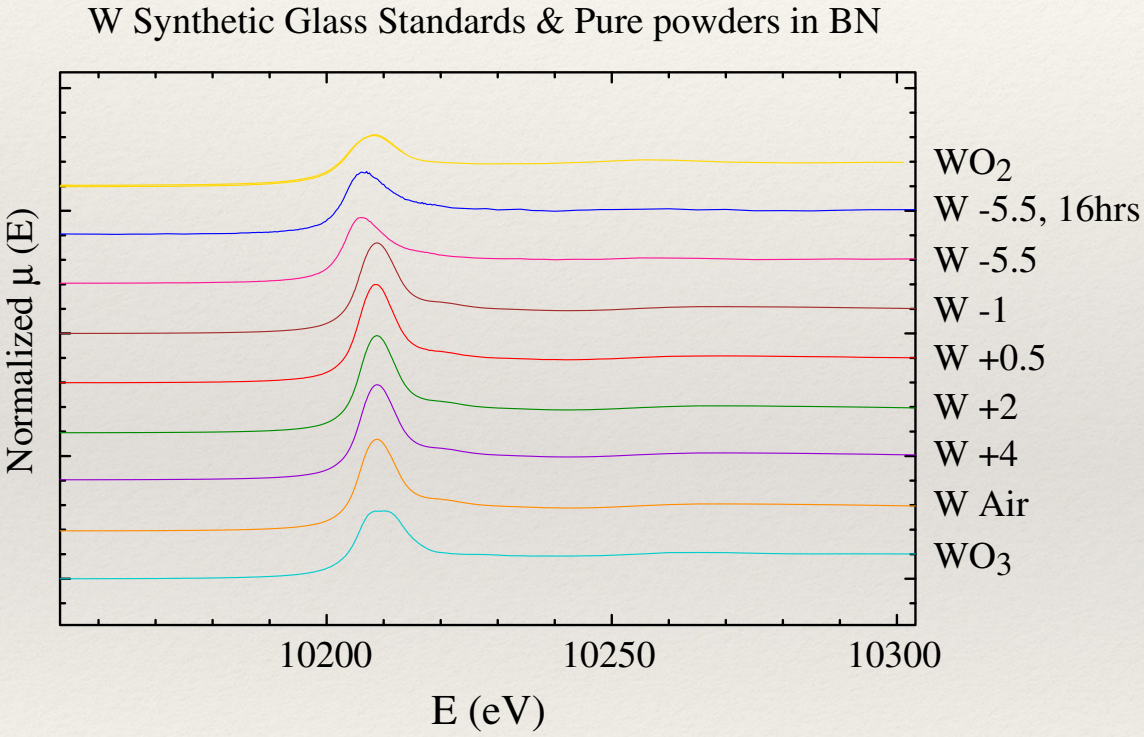

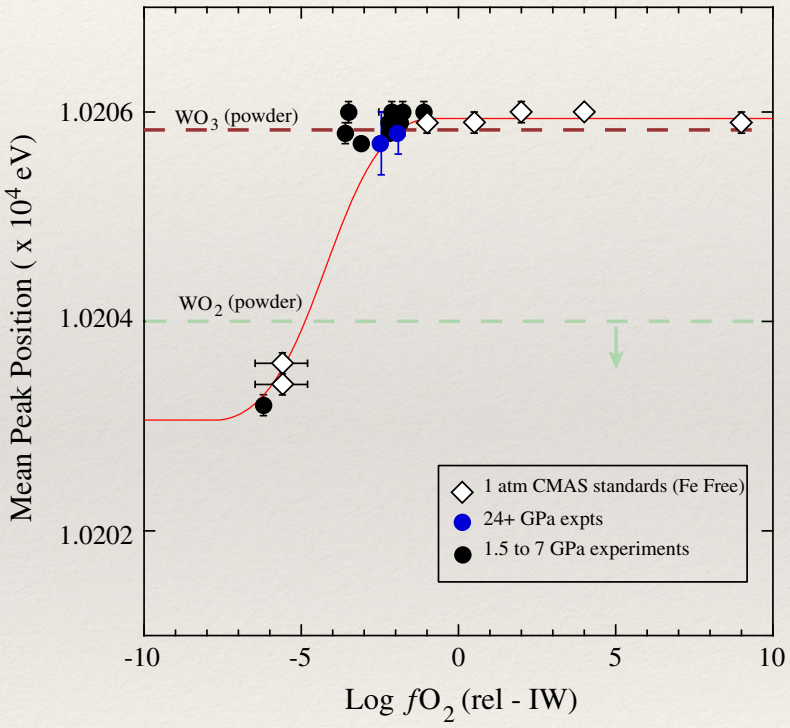

Change of W speciation with fO_2, no P-trend observed on quenched melts

The lattice strain model

- crystal chemistry: trace elements substitute to major cations of similar ionic radius

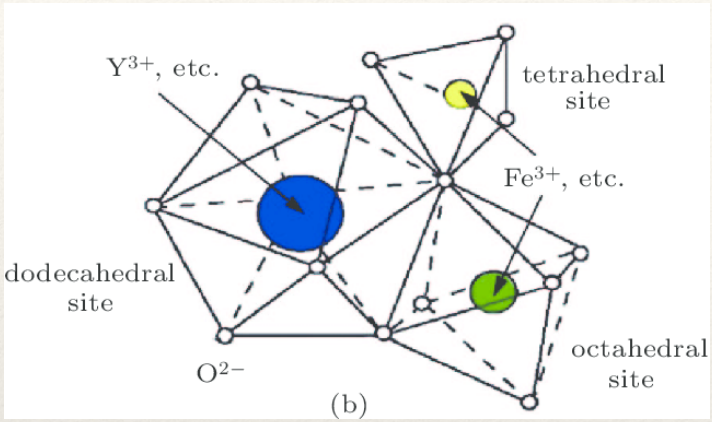

$$\Delta G_{strain} = 4\pi E\left(\frac{1}{2}\left(r_j - r_0\right)^2 + \frac{1}{3}\left(r_j - r_0\right)^3\right)$$

Brice Crystal Growth 1975

$$\epsilon = \frac{P}{E}$$

$$\int_{r_j}^{\infty} d\epsilon, dr = r_j - r_0$$

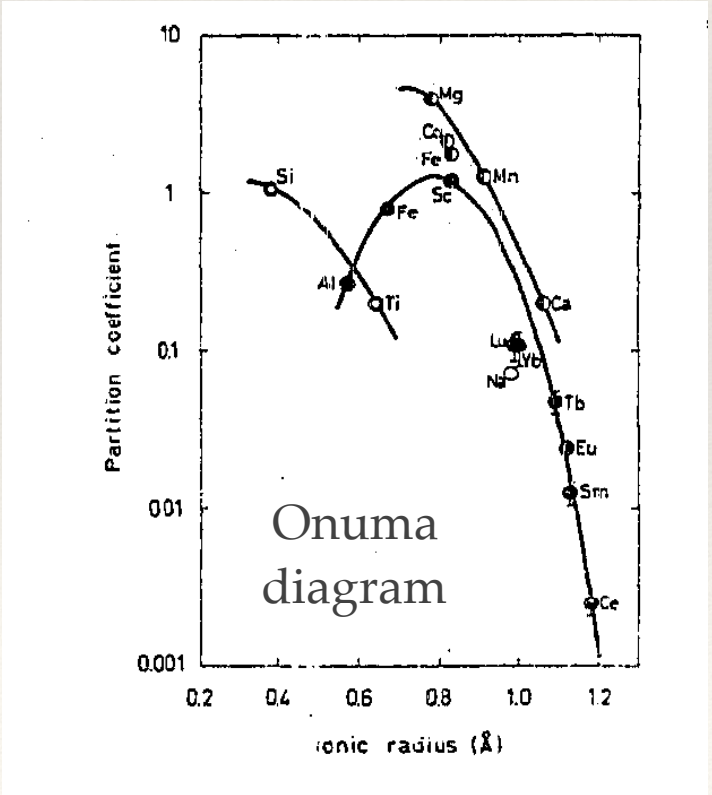

Onuma et al. EPSL 1968

The lattice strain model

- crystal chemistry: trace elements substitute to major cations of similar ionic radius

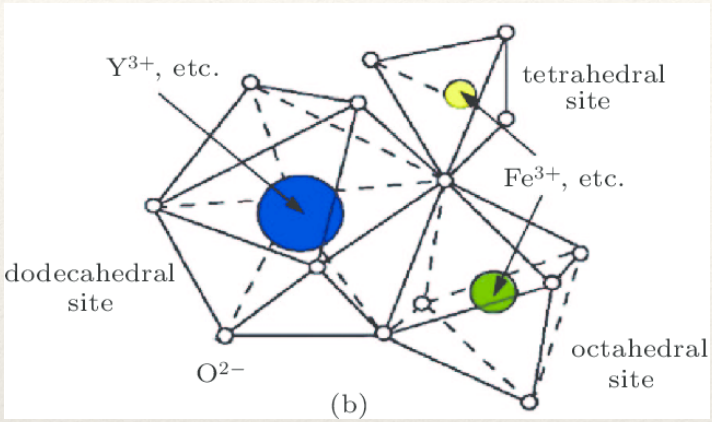

$$\Delta G_{strain} = 4\pi E\left(\frac{1}{2}\left(r_j - r_0\right)^2 + \frac{1}{3}\left(r_j - r_0\right)^3\right)$$

Brice Crystal Growth 1975

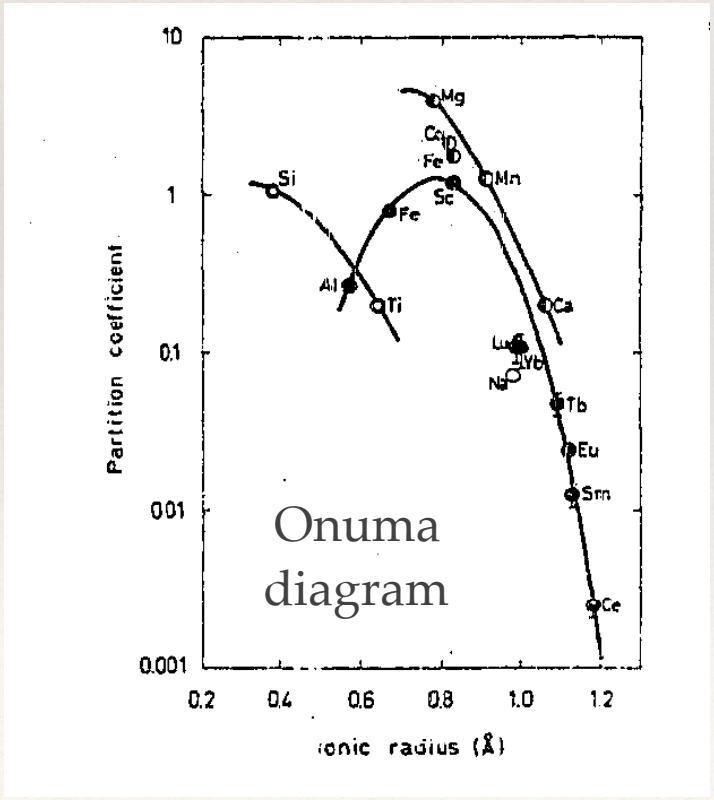

Onuma et al. EPSL 1968

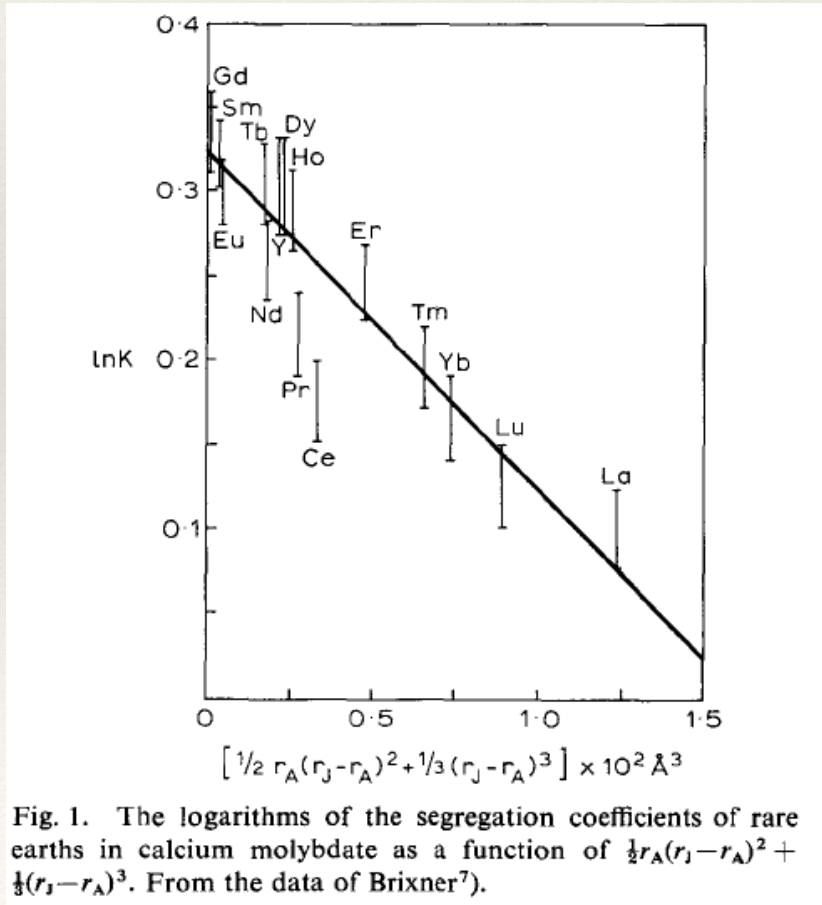

Fig. 1. The logarithms of the segregation coefficients of rare earths in calcium molybdate as a function of $\frac{1}{2}r_A(r_j - r_A)^2 + \frac{1}{3}(r_j - r_A)^3$. From the data of Brixner[7]).

The lattice strain model

- thermodynamic formalism:

$$\frac{x_M^{olivine}}{x_M^{melt}} = D_M^{olivine/melt}(T,P) = D_{Mg}\exp\left(-\frac{\Delta G_0}{RT}\right)$$

- Brice: calculated the strain associated to the insertion of a dopant in a crystal

$$\Delta G_{strain} = 4\pi E\left(\frac{1}{2}\left(r_j - r_0\right)^2 + \frac{1}{3}\left(r_j - r_0\right)^3\right)$$

Brice Crystal Growth 1975

- by assuming no strain in the melt:

$$D_i = D_0\exp\left(\frac{-4\pi E N_A\left(\frac{r_0}{2}(r_i - r_0)^2 + \frac{1}{3}(r_i - r_0)^3\right)}{RT}\right)$$

Blundy and Wood Nature 1994

D_0, the strain-free partition coefficient of a cation having the radius r_0

The lattice strain model

Blundy and Wood Nature 1994

$$D_i = D_0 \exp\left(\frac{-4\pi E N_A \left(\frac{r_0}{2}(r_i - r_0)^2 + \frac{1}{3}(r_i - r_0)^3\right)}{RT}\right)$$

- E related to bulk modulus

$$E = 3K_T(1 - 2\nu) \sim 1.5K_T$$

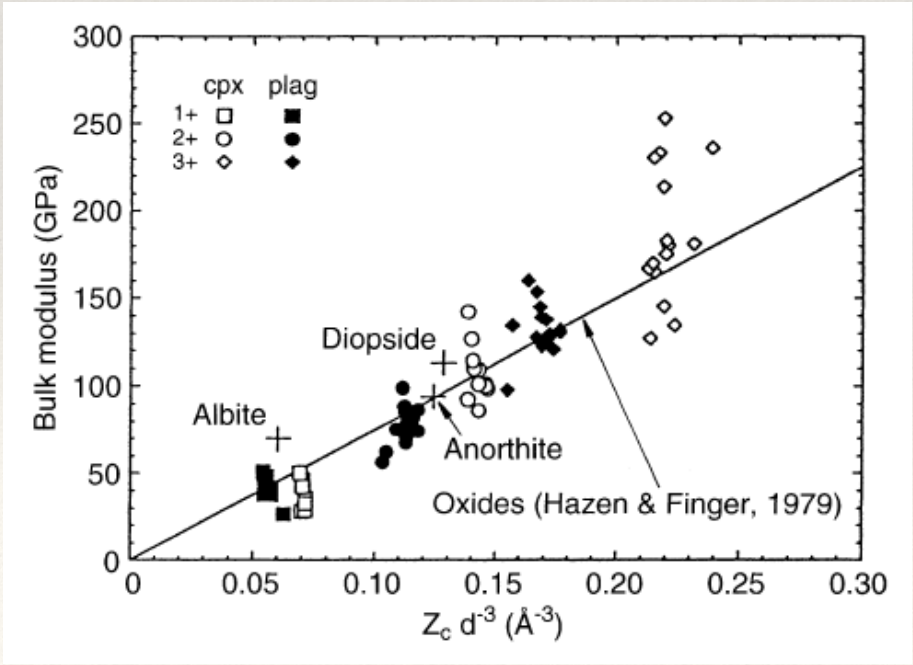

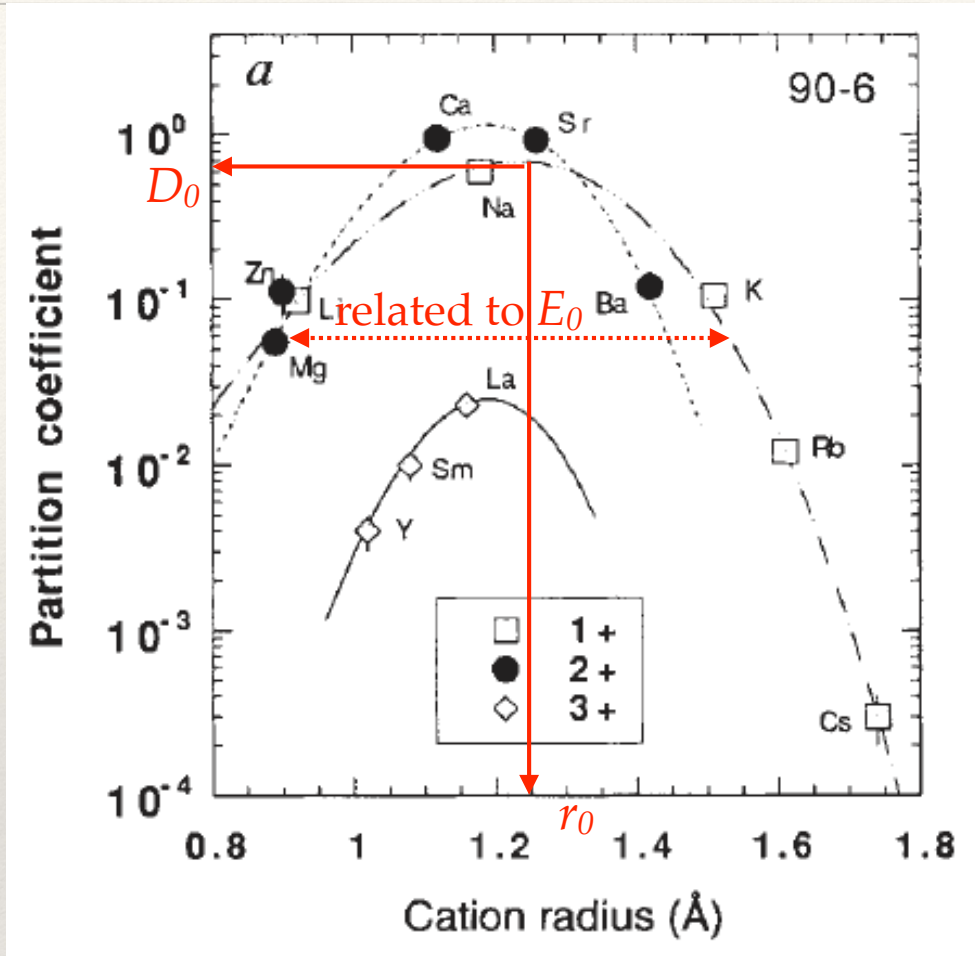

The lattice strain model

- refinement: D_0, E and r_0 as a function of P, T, composition

$$D_i = D_0 \exp\left(\frac{-4\pi E N_A \left(\frac{r_0}{2}(r_i - r_0)^2 + \frac{1}{3}(r_i - r_0)^3\right)}{RT}\right)$$

$r_0(3+)$ [Å]	=	$0.930 \cdot X_{Py} + 0.993 \cdot X_{Gr} + 0.916 \cdot X_{Alm} + 0.946 \cdot X_{Spes} + 1.05 \cdot (X_{And} + X_{Uv})$ $-0.005 \cdot (P$ [GPa]$-3.0)$
$E_X(3+)$ [GPa]	=	$3.5 \cdot 10^{12} \cdot (1.38 + r_0(3+)[\text{Å}])^{-26.7}$
$D_0(3+)$	=	$\frac{\exp\left(\frac{418000+10400 \cdot P[\text{GPa}]-226 \cdot T[\text{K}]}{8.314 \cdot T[\text{K}]}\right)}{\left(\gamma_{Mg}^{garnet} D_{Mg}\right)^2}$
γ_{Mg}^{garnet}	=	$\exp\left(\frac{19000 \cdot X_{Ca}^2}{8.314 \cdot T[\text{K}]}\right)$

van Westrenen et al. Contrib. 2001

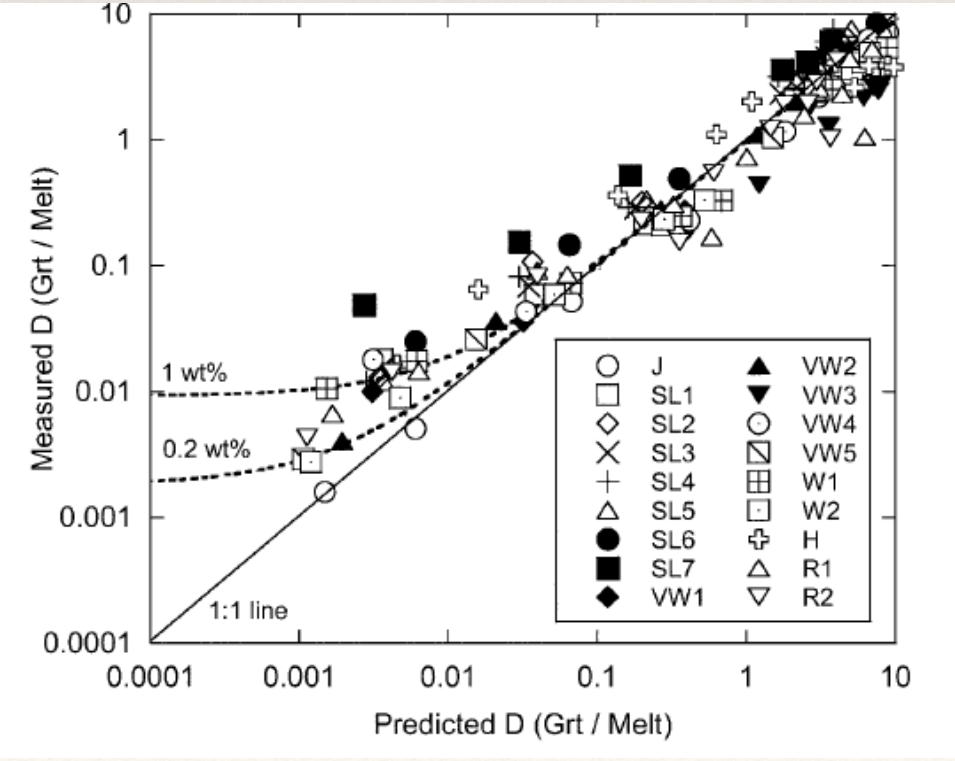

Sun and Liang Chem. Geol. 2013

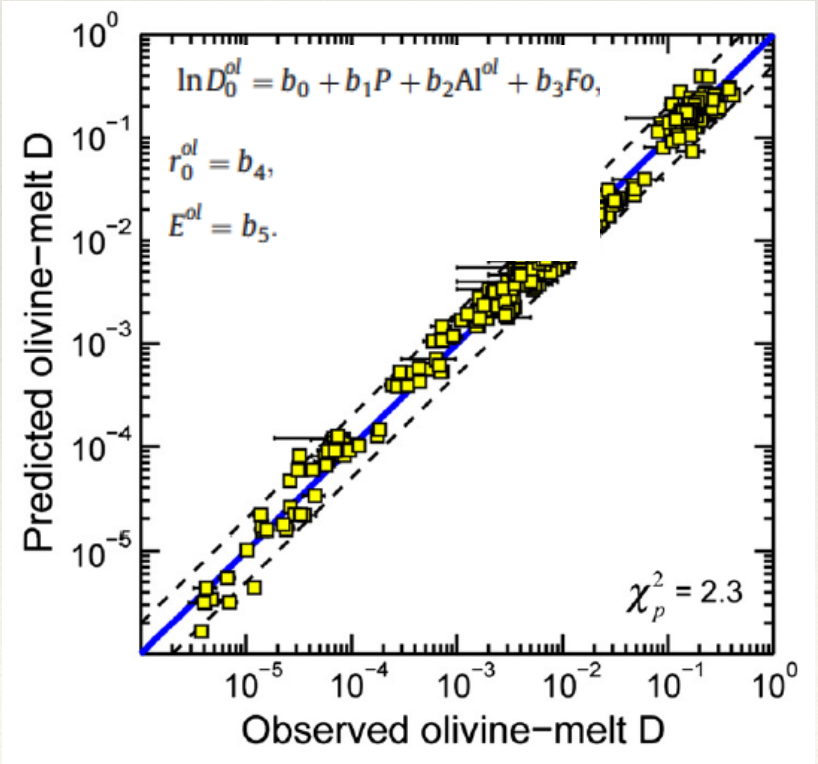

Importance of melt structure

Pb: Site elasticity should increase with P

Majorite / melt partitioning

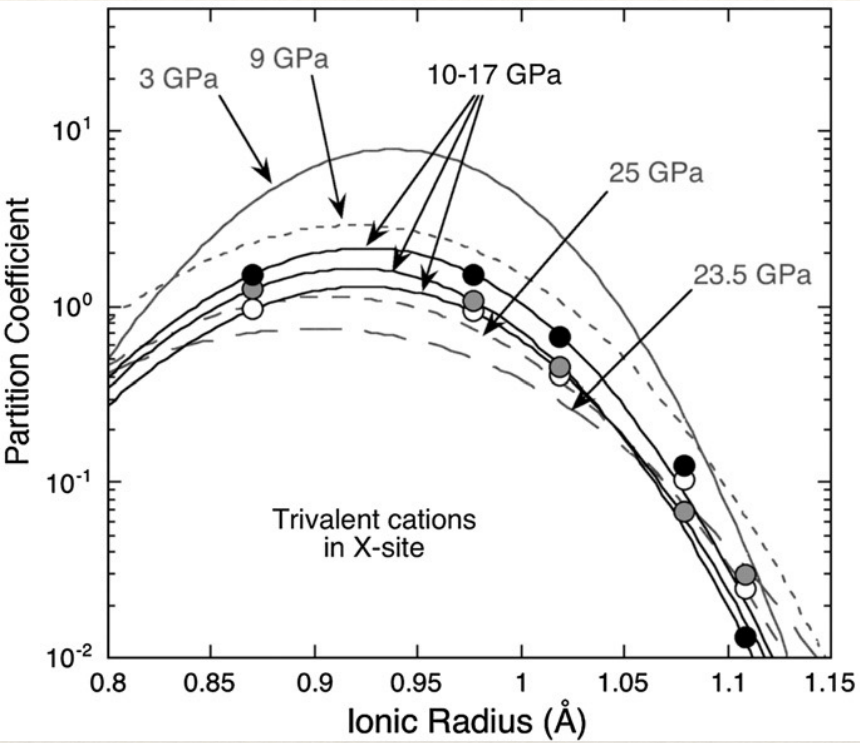

Corgne et al. Lithos 2012

Olivine / melt partitioning

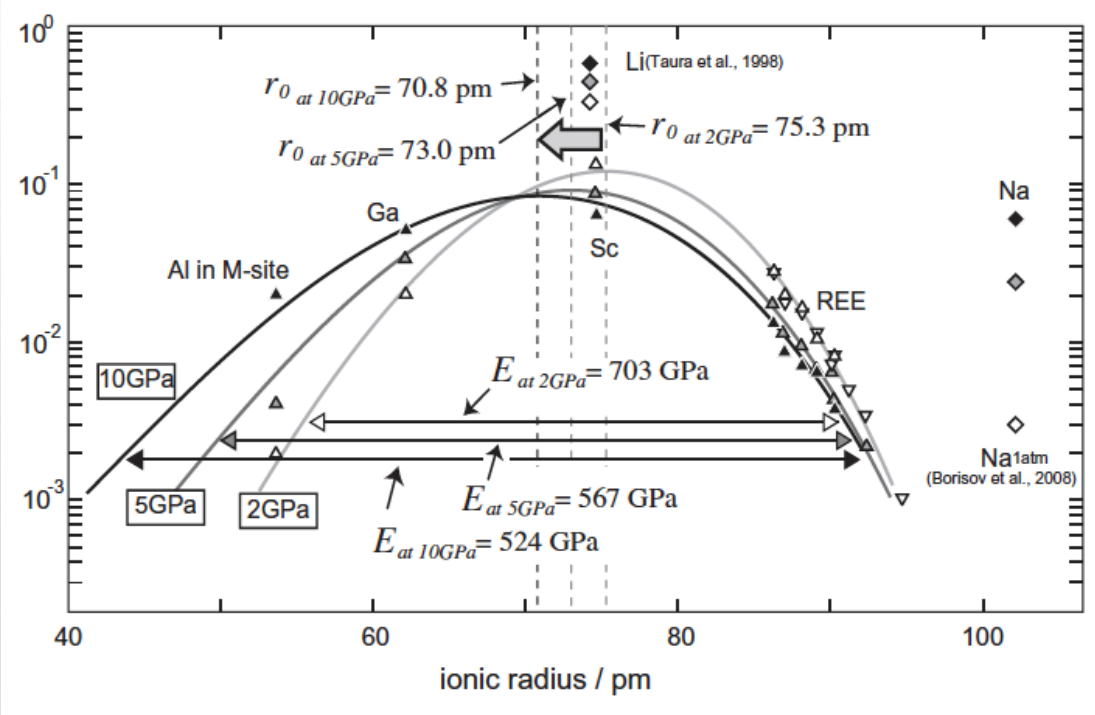

Imai et al. PEPI 2012

$$D_i * (P,T,X) = D_0(P,T,X) \times \exp\left[\frac{-4\pi N_A}{RT}(E_{\text{olivine}} - E_{\text{melt}})\left(\frac{r_0}{2}(r_i - r_0)^2 + \frac{1}{3}(r_i - r_0)^3\right)\right]$$

- limitation of the lattice strain model: does not take into account melt's properties

Importance of melt structure

- Test of the influence of melt structure: case of melt-melt immiscibility ⇒ melt composition (*i.e.* degree of polymerization) controls element partitioning

Schmidt et al. Science 2016

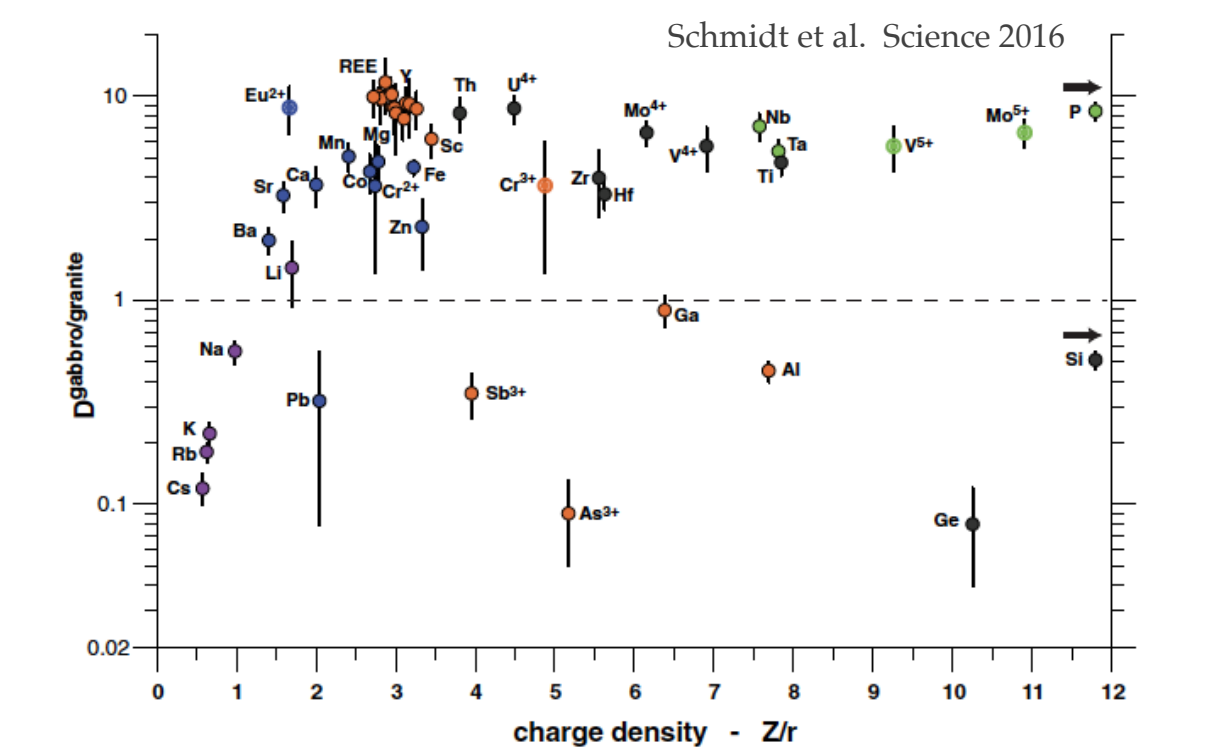

0.3-0.7 GPa / 1100-1240°C

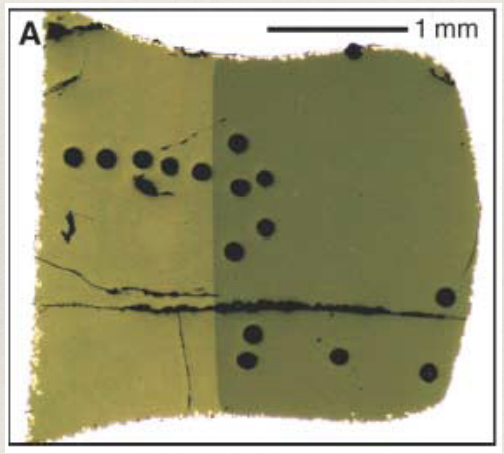

Importance of melt structure

- Test of the influence of melt structure: case of melt-melt immiscibility ⇒ melt composition (*i.e.* degree of polymerization) controls element partitioning

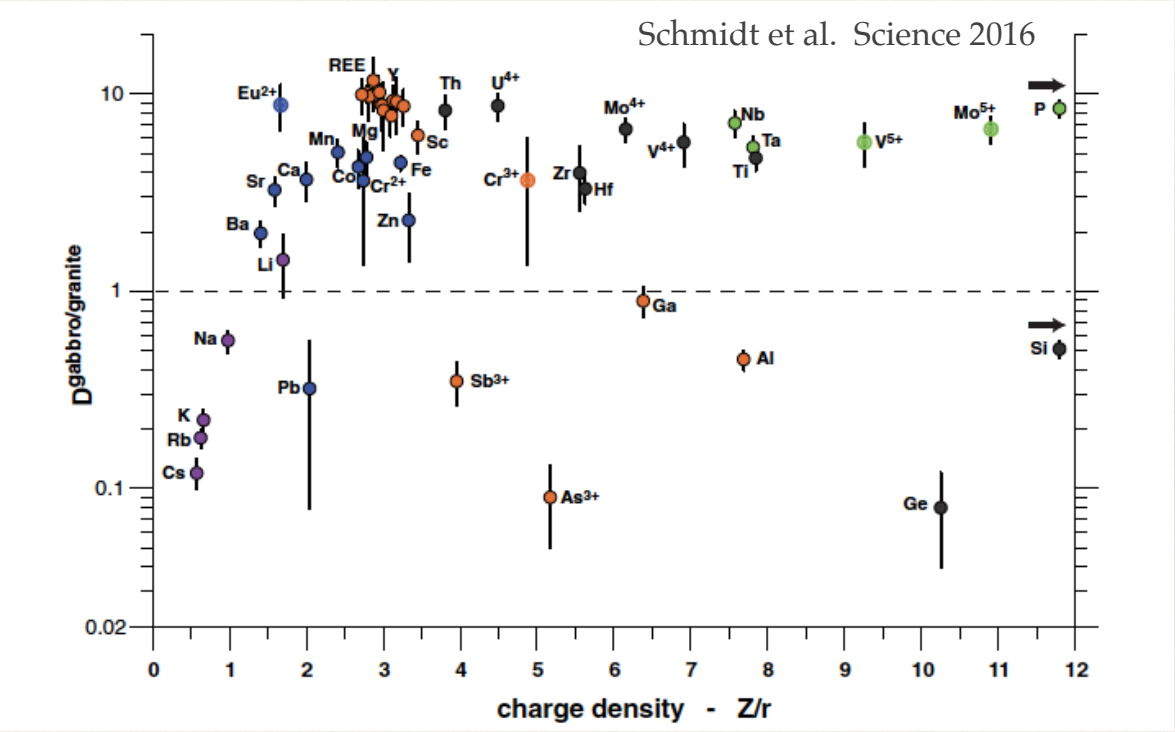

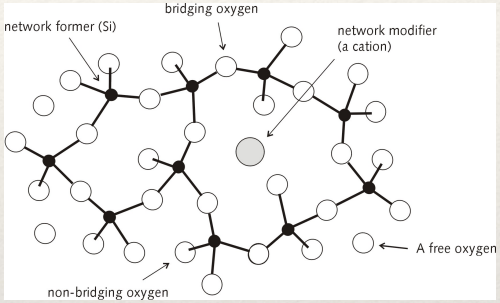

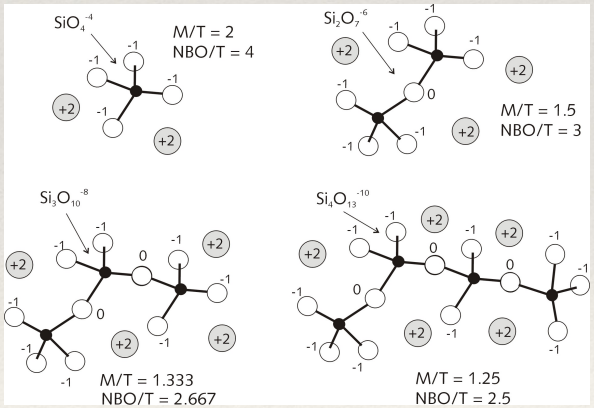

Importance of melt structure

- influence of melt structure: case of melt-melt immiscibility high pressure experiments using a centrifuging piston-cylinder press (ETHZ)

Influence of melt structure on partitioning

- influence of melt structure: case of melt-melt immiscibility
  ⇒ melt composition (*i.e.* degree of polymerization) controls element partitioning

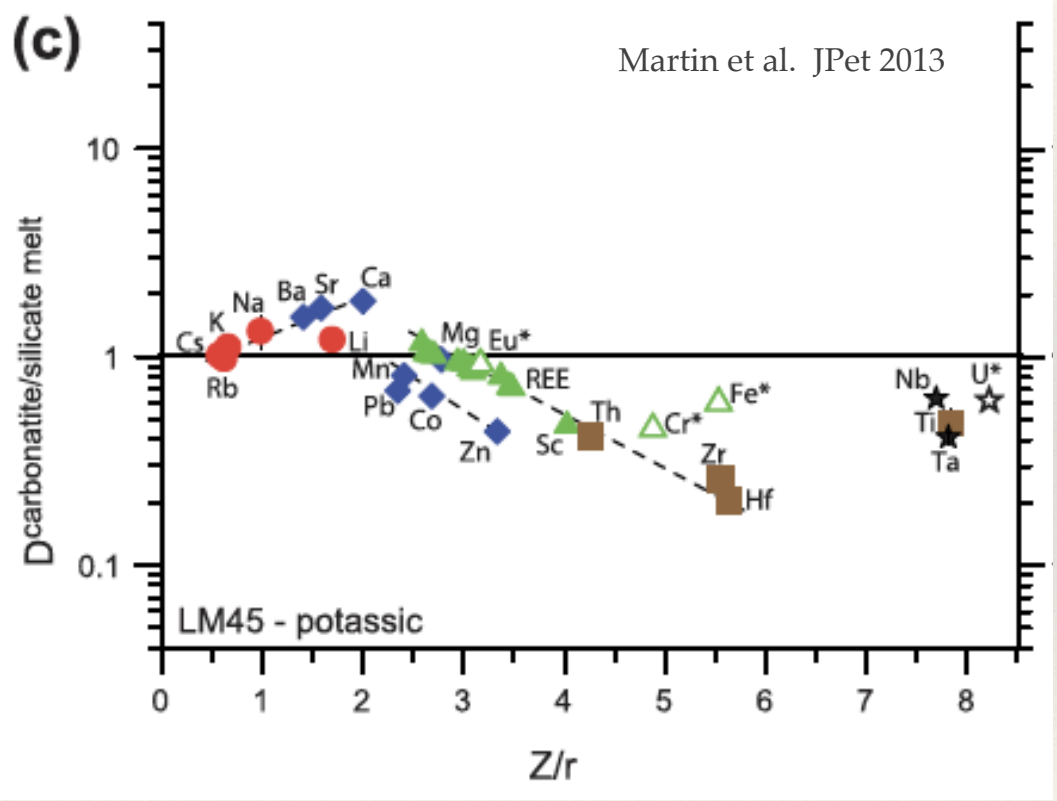

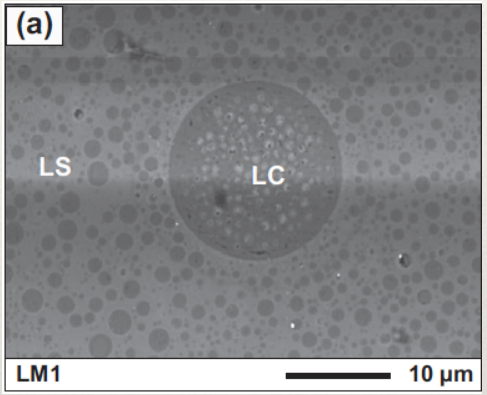

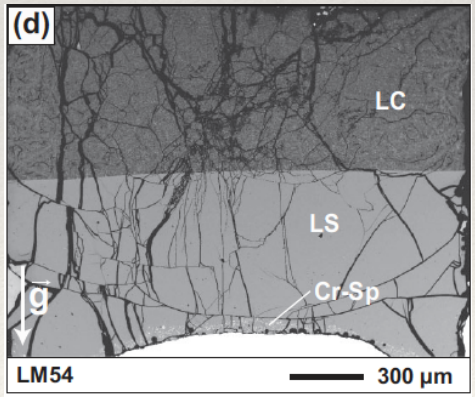

Influence of melt structure on partitioning

- Structure of silicate melts: rings and cavities

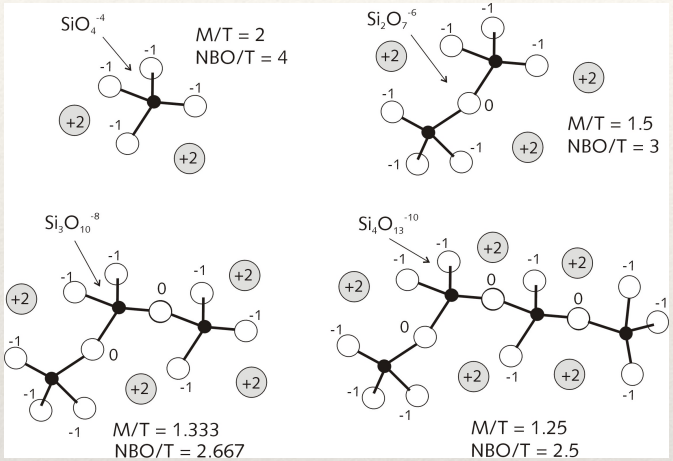

SEM image SiO_2 glass monolayer

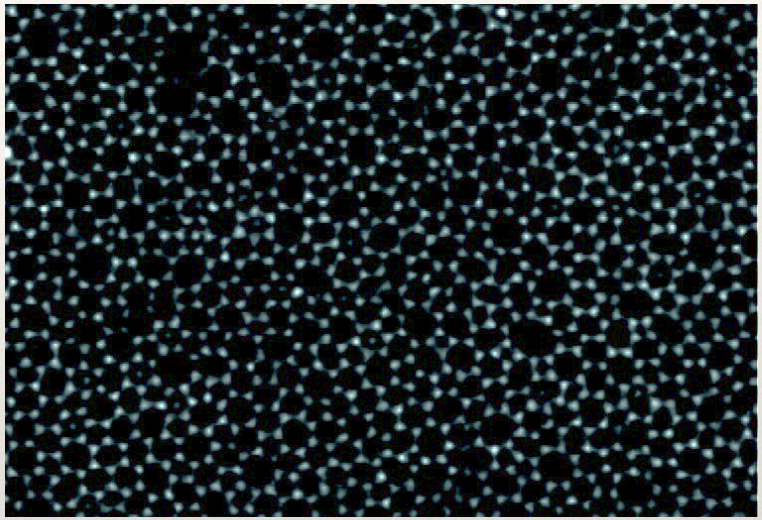

Huang et al. Nano Lett. 2012

- Structure of mantle silicates

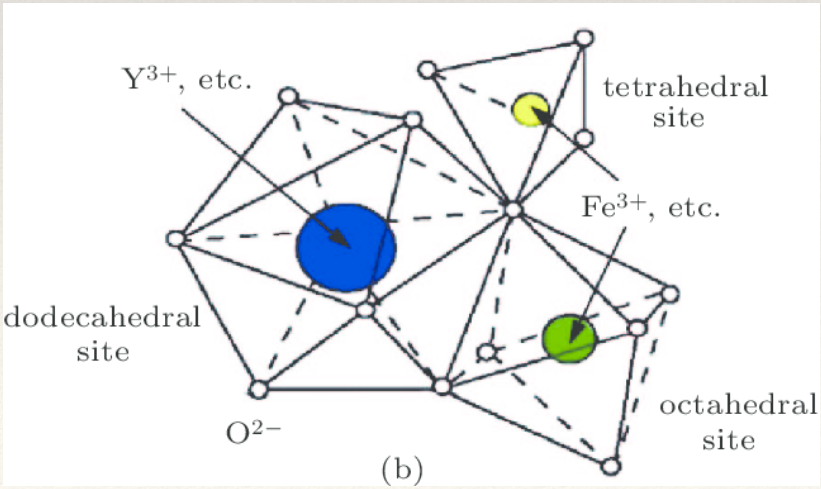

Influence of melt structure on partitioning

- molecular dynamics: can work with relatively large number of atoms (unlike full ab initio), still 1000-2000 maximum *i.e.* 0.1 at% minimum

$$Y^{3+}_{granite} + Al^{3+}_{gabbro} \rightleftharpoons Al^{3+}_{granite} + Y^{3+}_{gabbro}$$

$$\Delta G^{exc} = \Delta F^{Y\rightarrow Al}_{granite} - \Delta F^{Y\rightarrow Al}_{gabbro}$$

$$K_{exc} \cdot \frac{\gamma^{Al}_{gabbro}\gamma^{Y}_{granite}}{\gamma^{Y}_{gabbro}\gamma^{Al}_{granite}} = \frac{[Y_{gabbro}][Al_{granite}]}{[Al_{gabbro}][Y_{granite}]}$$

$$K_{exc} \approx D_Y^{gabbro/granite} = \frac{[Y_{gabbro}]}{[Y_{granite}]}$$

Melt pair & element	T_{exc} (K)	ΔG_{exc} (kJ/mol)	K_{exc} (D_{exc})	D_{est}	D_{exp}	T_{exp} (K)
			classical MD			
gab/gra Y	2500	−26	3.4	8	9.3(18)[b]	1450
gab/gra Y^{super}	2500	−29	4.0	10		
gab/gra 2Y	2500	−30	4.2	12		
gab/gra $2Y^{super}$	2500	−31	4.4	13		
gab/gra La	2500	−24	3.2	7	9.9(19)[b]	1450
			first-principles MD			
gab/gra Y a	3000	−3	1.1	1.2	9.3(18)[b]	1450
gab/gra Y b	3000	3	0.9	0.8		
gab/gra As	3000	29	0.3	0.09	0.086(52)[b]	1450
asi200/asi280 Y	3000	−31	3.5	15[a]	∼502[c,a]	1400

Haigis et al. GCA 2013, Wagner et al. GCA 2017

Influence of melt structure on partitioning

- molecular dynamics: structural insights corroborate EXAFS data, *i.e.* Y bonding in melts changes with polymerization

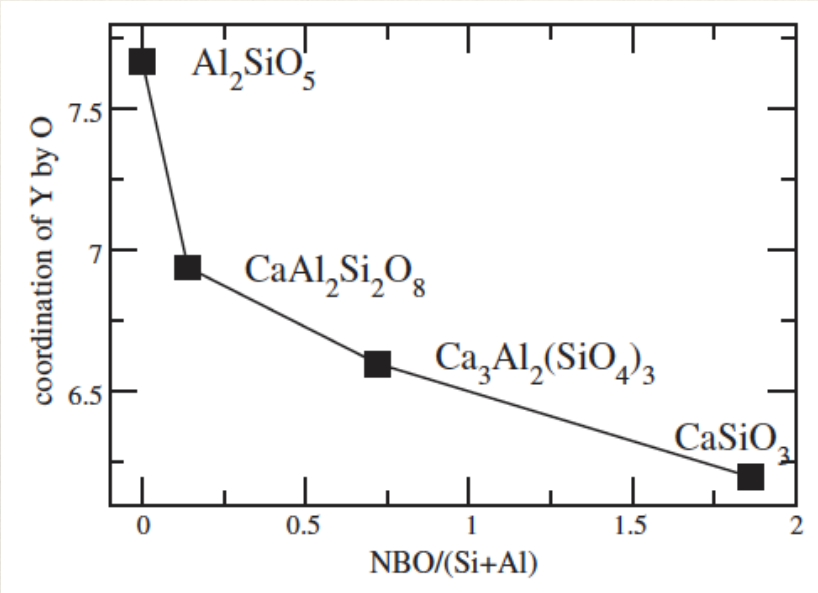

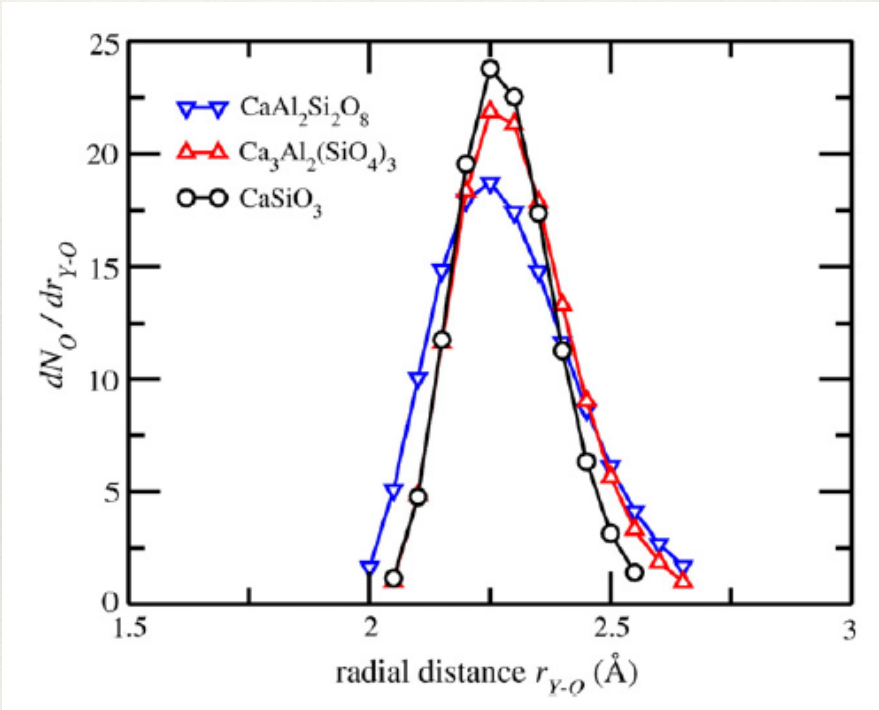

Haigis et al. GCA 2013

Influence of melt structure on partitioning

- Melt compressibility changes with composition and P

Compilation of datasets, refs in de Grouchy et al. EPSL 2017

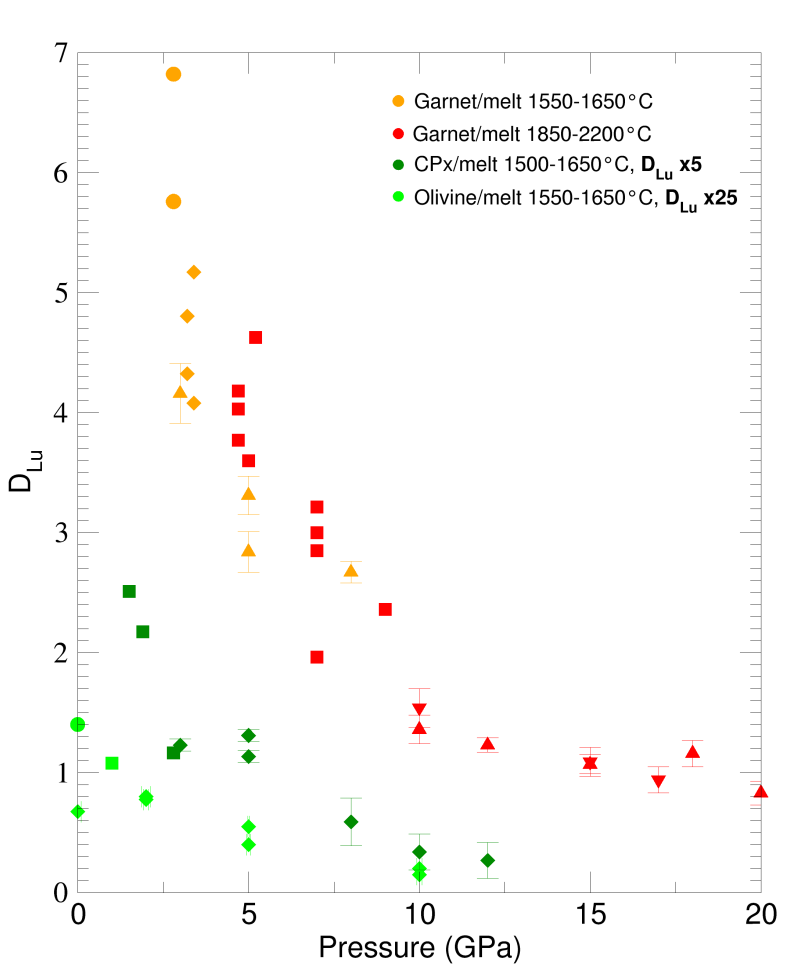

Sanloup Chem. Geol. 2016

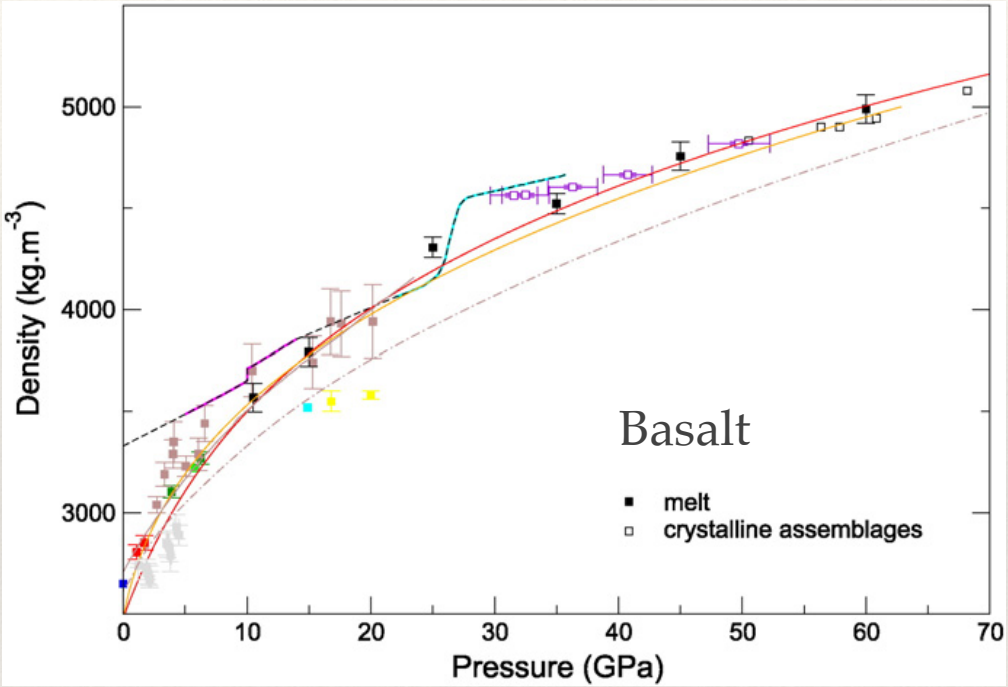

$$D_i * (P,T,X) = D_0(P,T,X) \times \exp\left[\frac{-4\pi N_A}{RT}(E_{\text{olivine}} - E_{\text{melt}})\left(\frac{r_0}{2}(r_i - r_0)^2 + \frac{1}{3}(r_i - r_0)^3\right)\right]$$

Imai et al. PEPI 2012

Influence of melt structure on partitioning

- Exploring melt structure under pressure

X-ray diffraction:
All elements contribute to signal
Restrictions: only very heavy elements

Resistive-heating DACs
and Paris-Edinburgh press

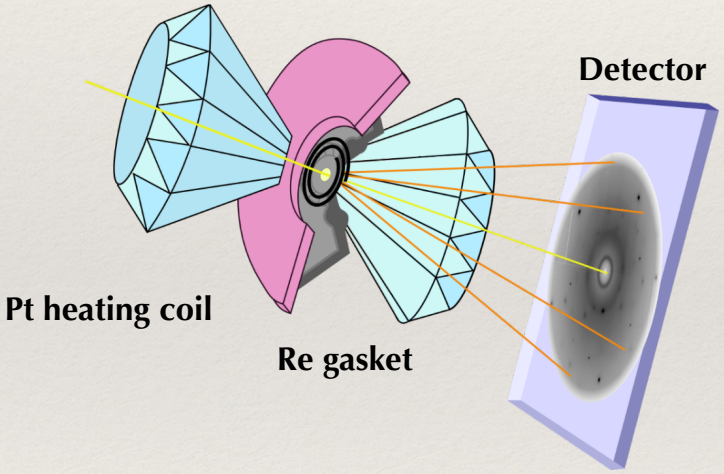

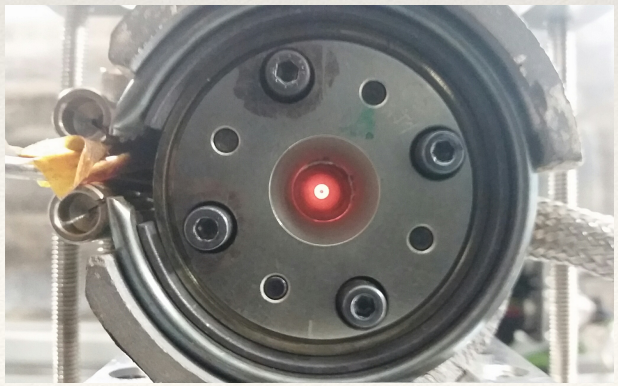

EXAFS/XANES:
Chemically selective, model dependent
Restrictions: energies>10 keV

Paris-Edinburgh press using
nanocristalline diamond capsules

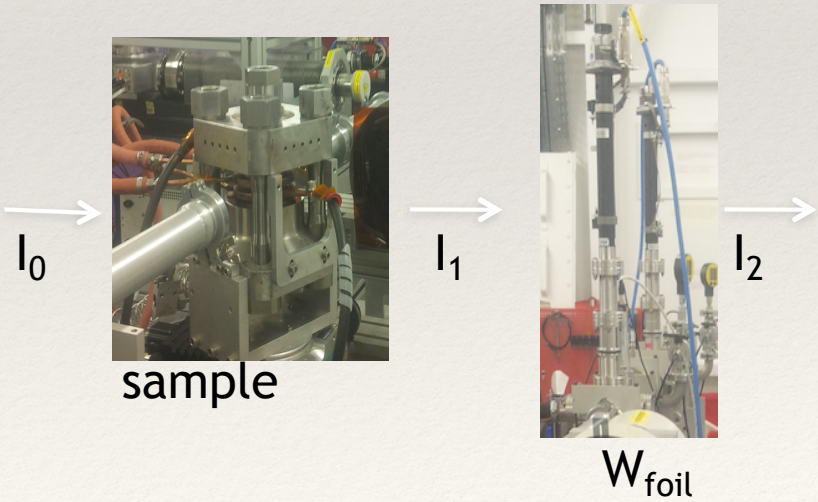

Influence of melt structure on partitioning

- Structure of liquids from angle dispersive X-ray diffraction

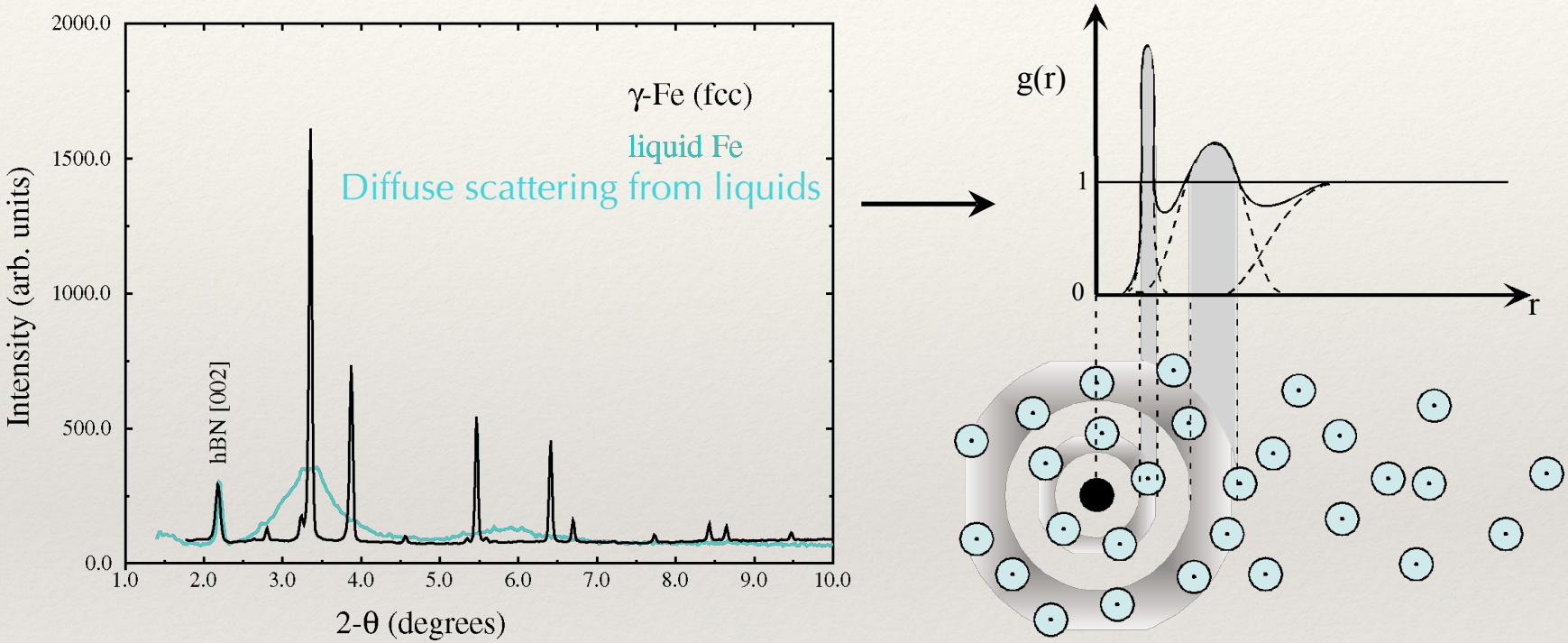

Radial distribution functions, g(r), describe the short range order: first interatomic distances (up to 5 Å) and coordination numbers

Influence of melt structure on partitioning

- Melt compressibility changes with P
- Trace elements local environment may change with P

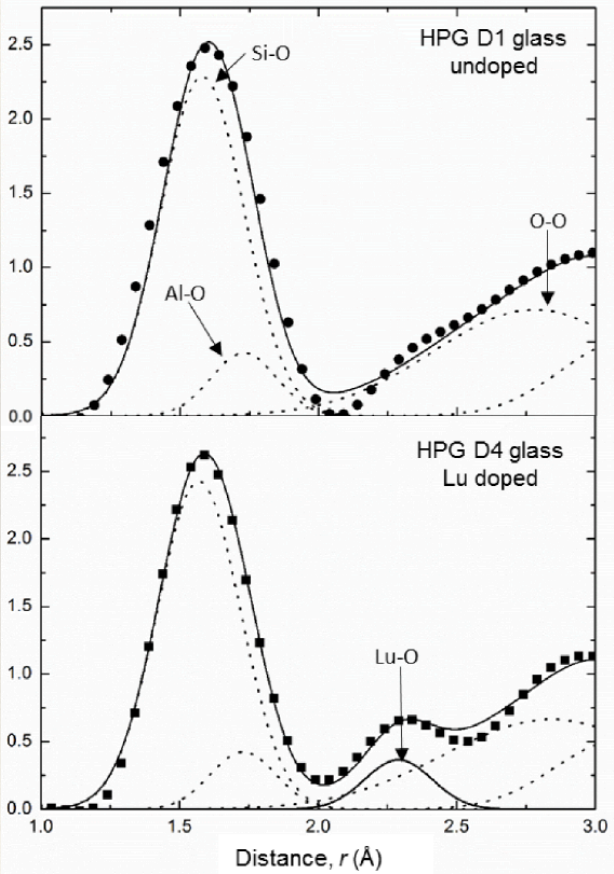

Radial distribution functions

HPG: Fe-free granite analogue

An-D: Fe-free basalt analogue

Lu-O coordination changes:

1) as a function of melt composition
2) as a function of P in basalt at 4-5 GPa

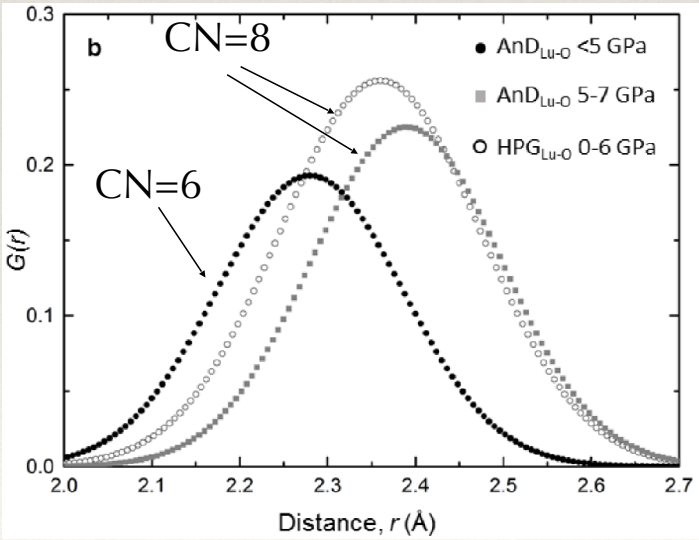

de Grouchy et al. EPSL 2017

Influence of melt structure on partitioning

- REE affected at different P threshold

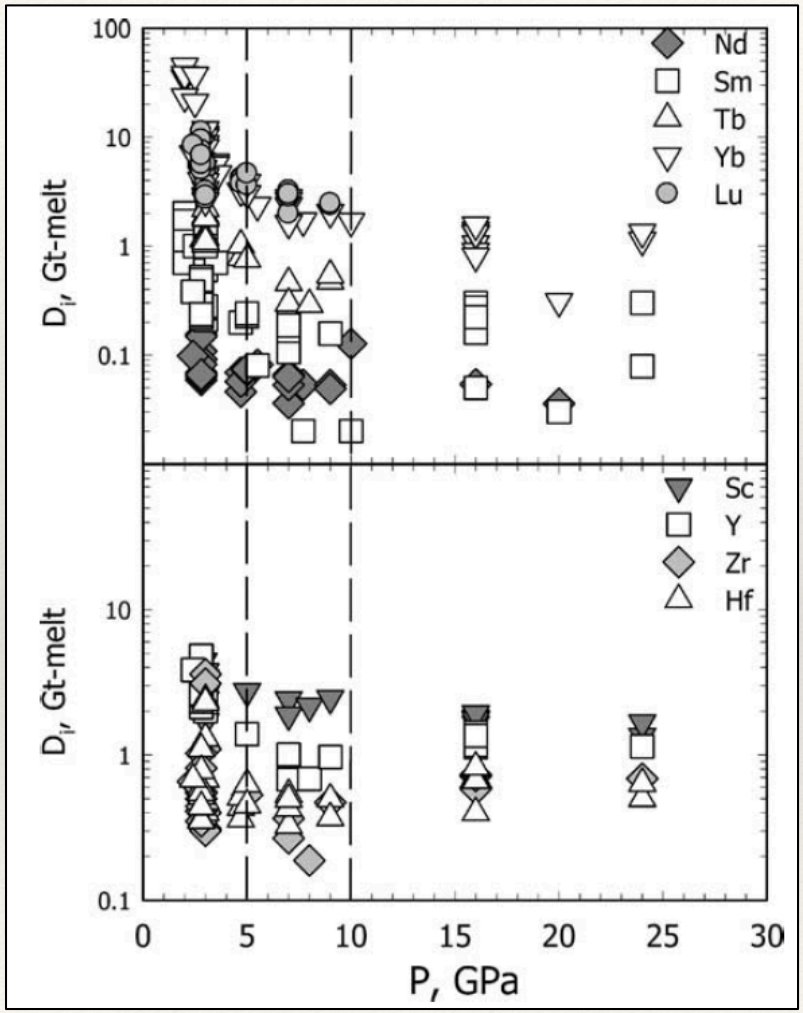

Draper et al. PEPI 2003

- Potentially linked to collapse of voids in the silicate melt structure

SEM image SiO_2 glass monolayer

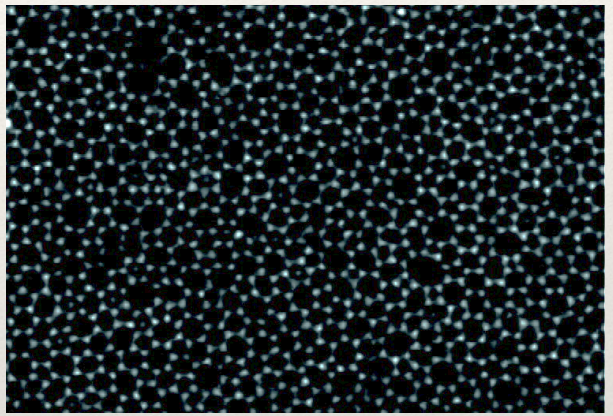

Huang et al. Nano Lett. 2012

⇒ Melt structure strongly influences element partitioning

⇒ D_{REE} decrease with P, for garnet: $D_{Lu}/D_{Hf} \rightarrow 1$

⇒ Decoupling of the Sm/Nd and Lu/Hf systems

Influence of melt structure on partitioning

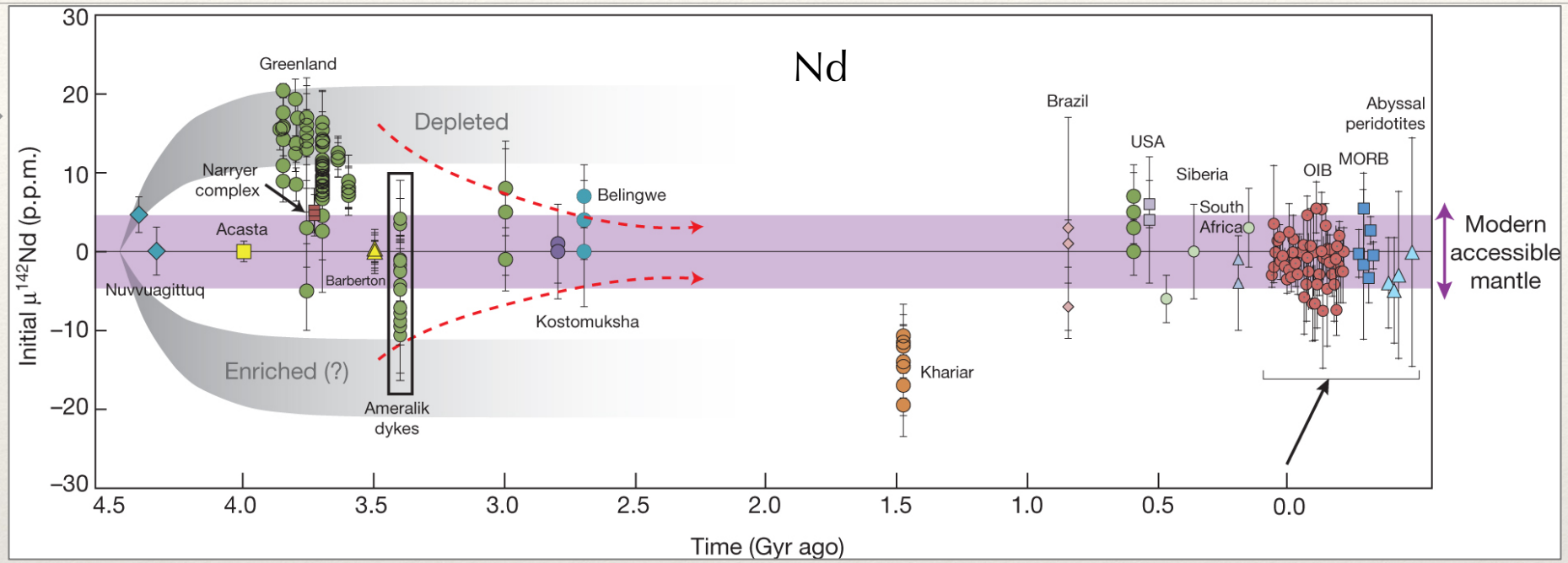

H Rizo et al. Nature 2012

Hf

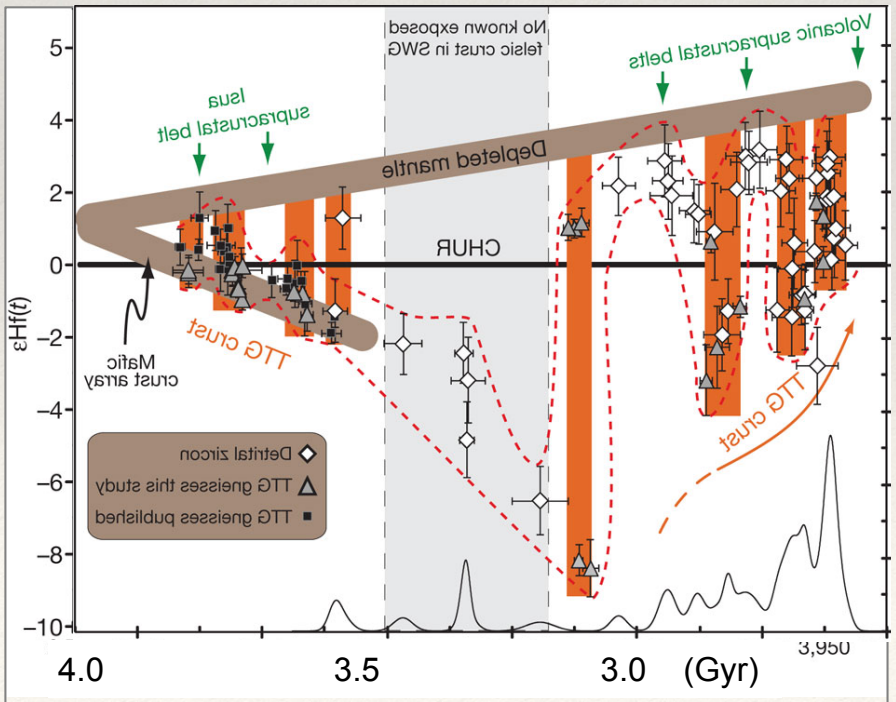

Næraa et al
Nature 2012

Different information from
Nd and Hf isotopes
on early crust formation

⇔ Decoupling of the Sm/Nd and
Lu/Hf systems at high P

Crystal/melt Fe partitioning

- basalts enrichment (and consequent easier to detect basalts/eclogites at depth)
- spin transition in deep mantle

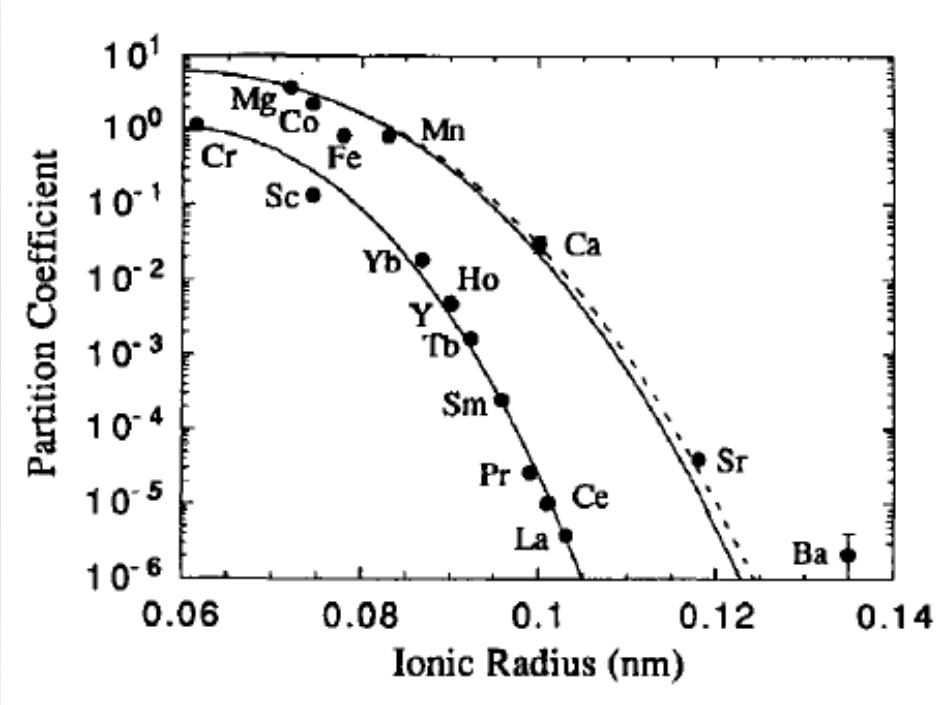

Problem with Fe: off the trend for olivine/melt
1463 K - 1 bar

Beattie Min. Mag. 1994

Crystal/melt Fe partitioning

- Continental lithosphere, colder but depleted in Fe ⇒ stabilized
- Dense LLSVP, Fe enriched ⇒ stabilized

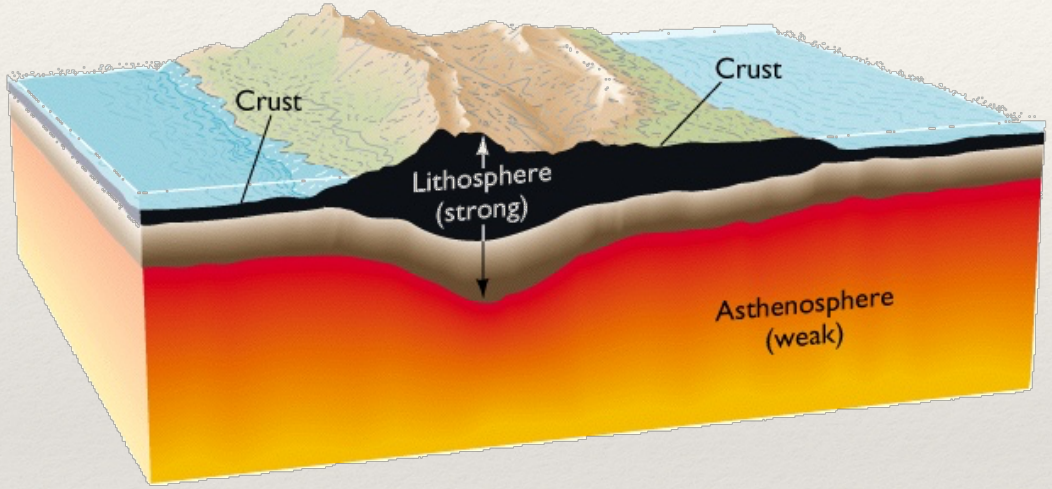

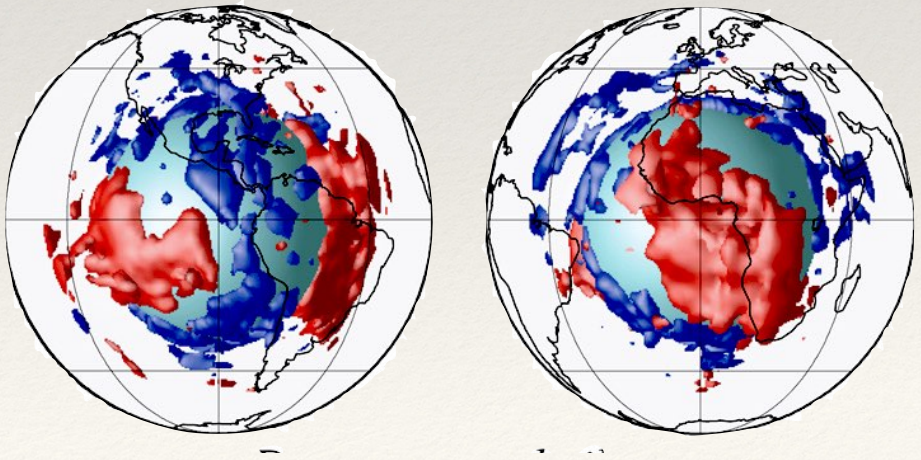

Crystal/melt Fe partitioning

- Fe behaviour during partial melting

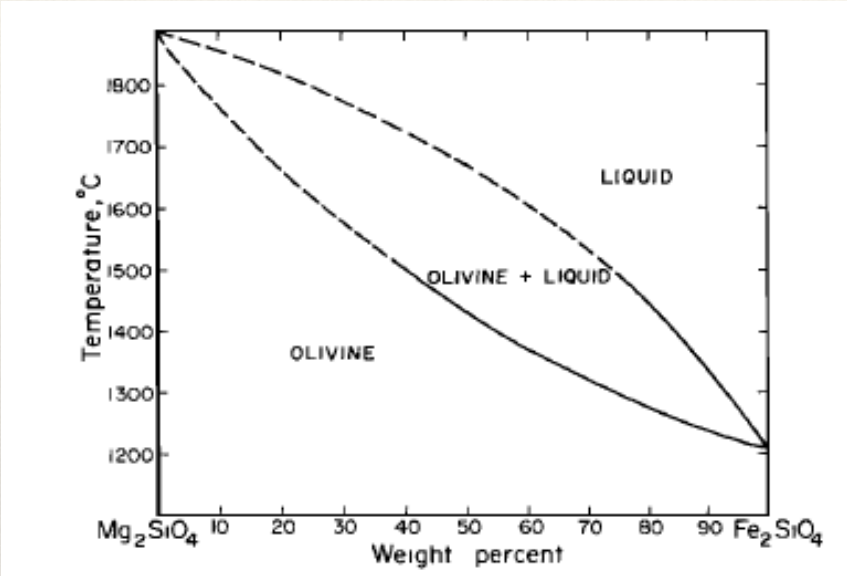

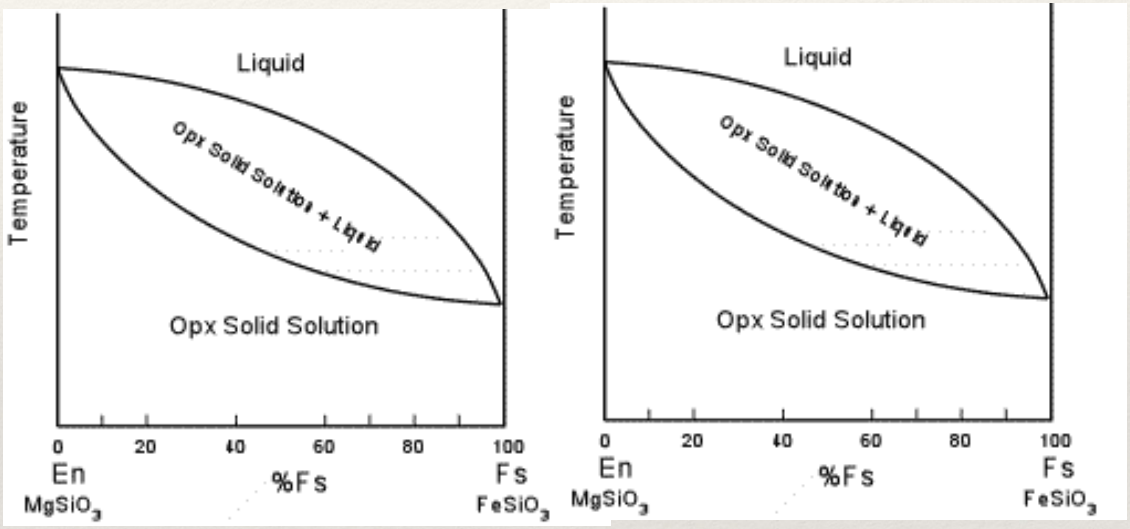

$$K_D = \frac{[FeO]/[MgO]_{mineral}}{[FeO]/[MgO]_{liquide}}$$

olivine K_D=0,3

pyroxene K_D=0,2-0,3

$\Rightarrow$ Partial melting of the mantle produces Fe-rich melts

Presnall AGU self book, from Bowen 1935

Crystal/melt Fe partitioning

- Reminder: pressure also increases MgO content

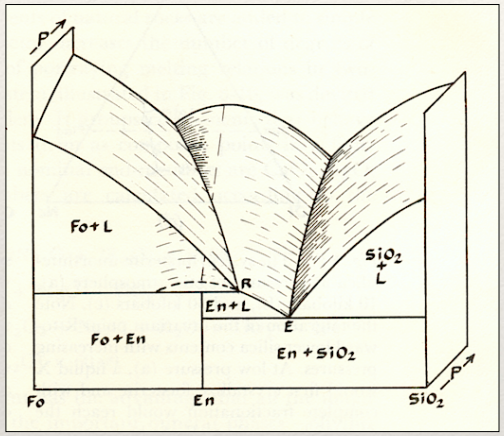

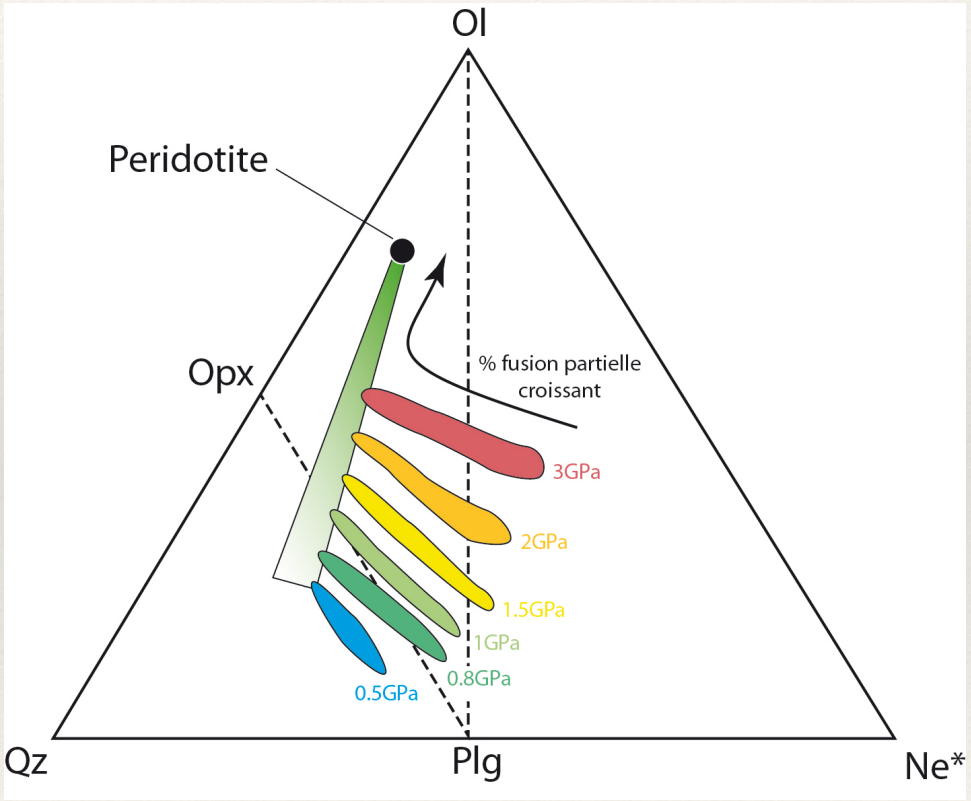

Crystal/melt Fe partitioning

- Fe behaviour during partial melting, effect of garnet at the residue

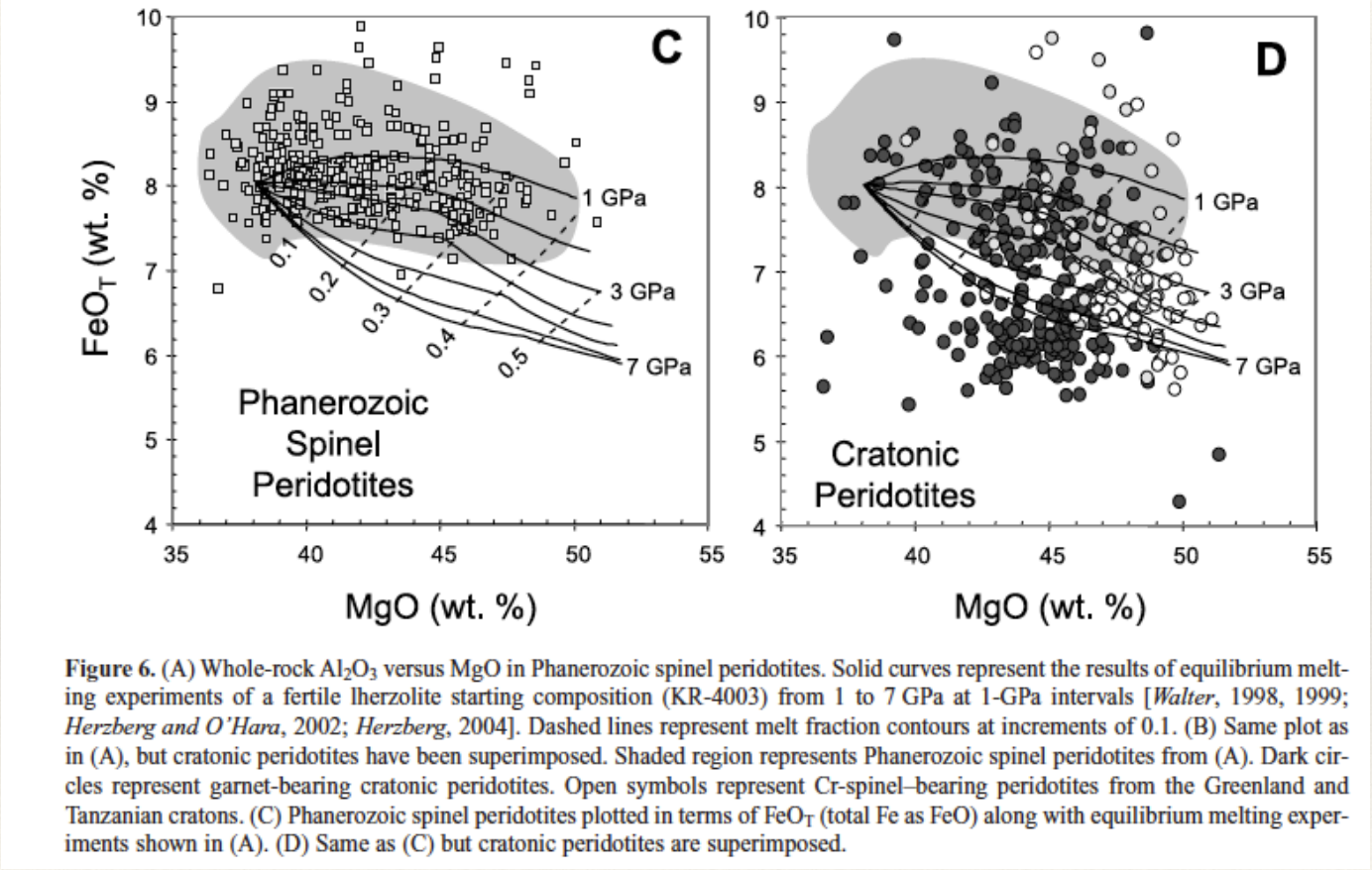

Figure 6. (A) Whole-rock Al_2O_3 versus MgO in Phanerozoic spinel peridotites. Solid curves represent the results of equilibrium melting experiments of a fertile lherzolite starting composition (KR-4003) from 1 to 7 GPa at 1-GPa intervals [*Walter*, 1998, 1999; *Herzberg and O'Hara*, 2002; *Herzberg*, 2004]. Dashed lines represent melt fraction contours at increments of 0.1. (B) Same plot as in (A), but cratonic peridotites have been superimposed. Shaded region represents Phanerozoic spinel peridotites from (A). Dark circles represent garnet-bearing cratonic peridotites. Open symbols represent Cr-spinel–bearing peridotites from the Greenland and Tanzanian cratons. (C) Phanerozoic spinel peridotites plotted in terms of FeO_T (total Fe as FeO) along with equilibrium melting experiments shown in (A). (D) Same as (C) but cratonic peridotites are superimposed.

Lee AGU shelfbook 2006

Crystal/melt Fe partitioning

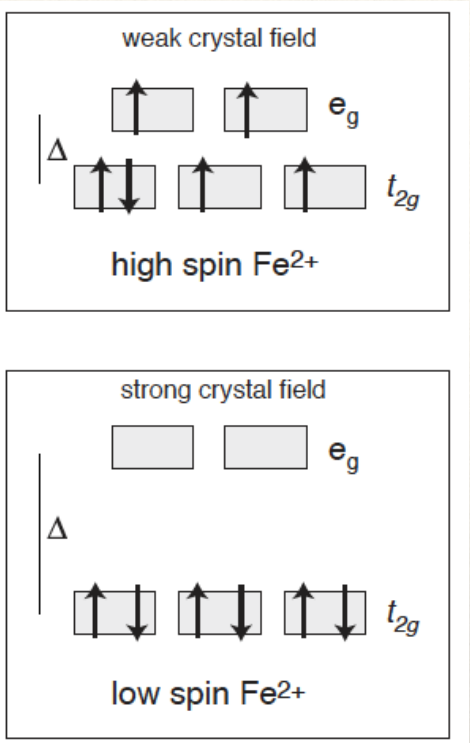

- Fe behaviour during partial melting persists in the lower mantle: no effect of the spin transition

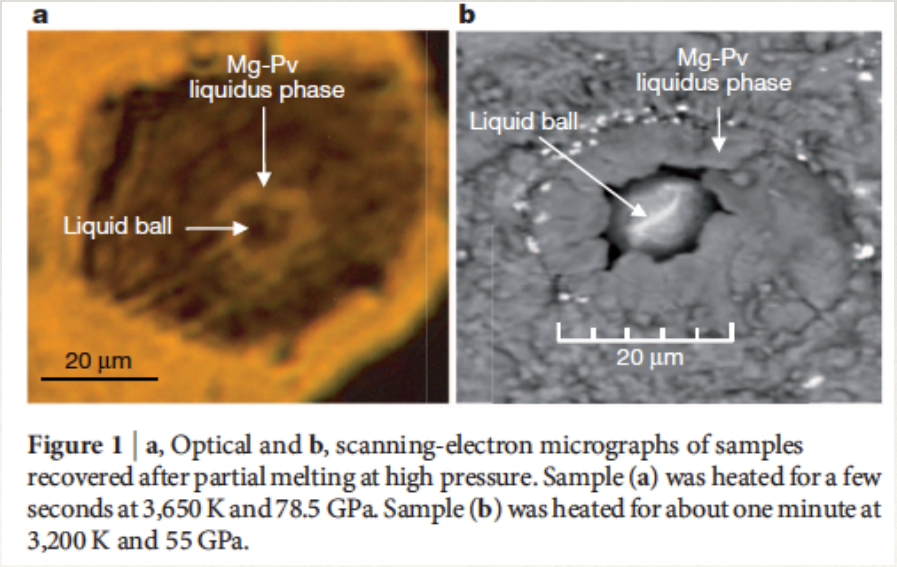

Figure 1 | **a**, Optical and **b**, scanning-electron micrographs of samples recovered after partial melting at high pressure. Sample (**a**) was heated for a few seconds at 3,650 K and 78.5 GPa. Sample (**b**) was heated for about one minute at 3,200 K and 55 GPa.

Andrault et al. Nature 2012

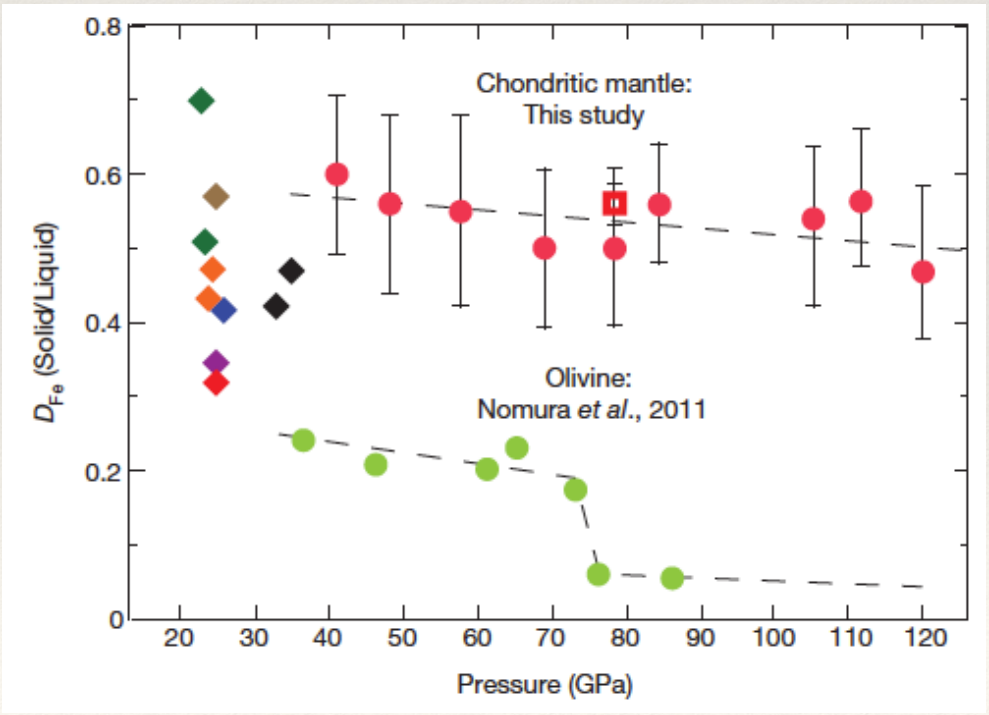

Crystal/melt Fe partitioning

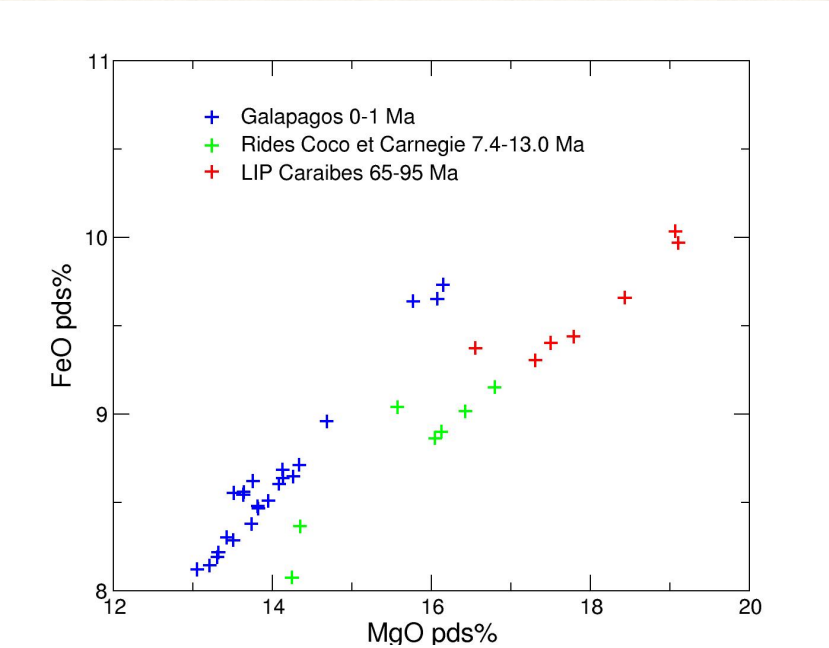

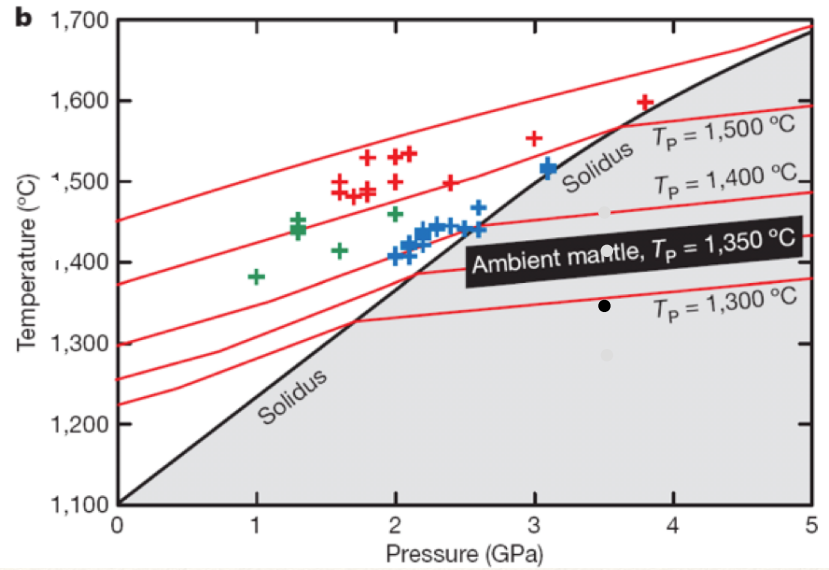

- Fe/Mg behaviour during partial melting: indicator of melting T

Herzberg&Gazel Nature 2009

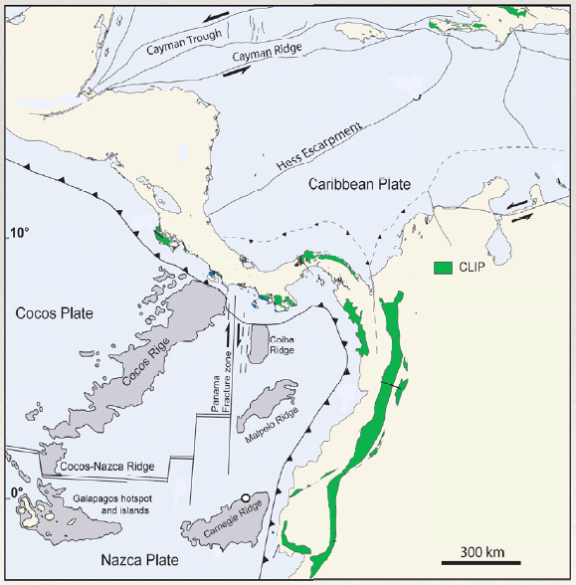

Crystal/melt Fe partitioning

- Fe/Mg behaviour during partial melting: indicator of melting T

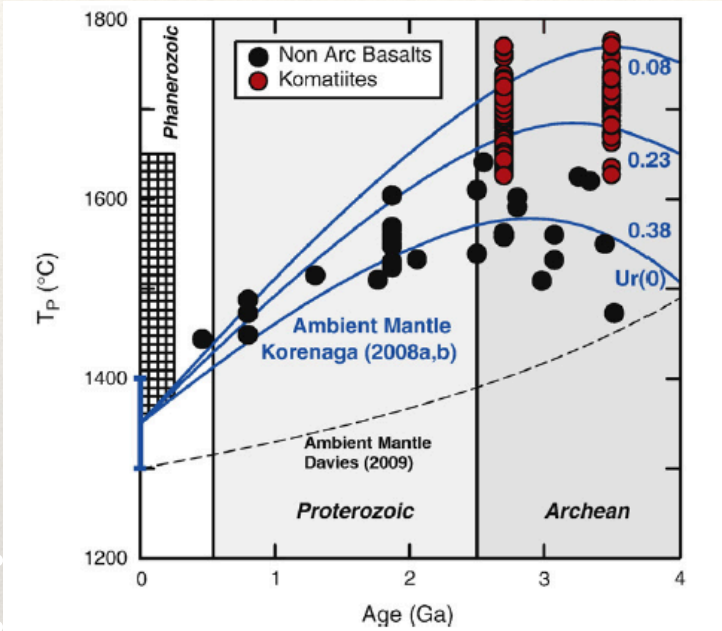

Fig. 1. Secular thermal Earth models for ambient mantle (blue curves; Korenaga, 2008a, b) compared with petrological estimates of mantle potential temperature (T_P) for non-arc lavas and komatiites with the ages indicated. Number next to each blue curve is the model present-day Urey ratio. We use the relation: $T_P(°C) = 1463 + 12.74MgO - 2924/MgO$ (Herzberg et al., 2007; Herzberg and Asimow, 2008), where MgO is the primary magma MgO content given in Table A1. The range of T_P for plume-related magmas of Phanerozoic age is from Herzberg and Asimow (2008) and Herzberg and Gazel (2009).

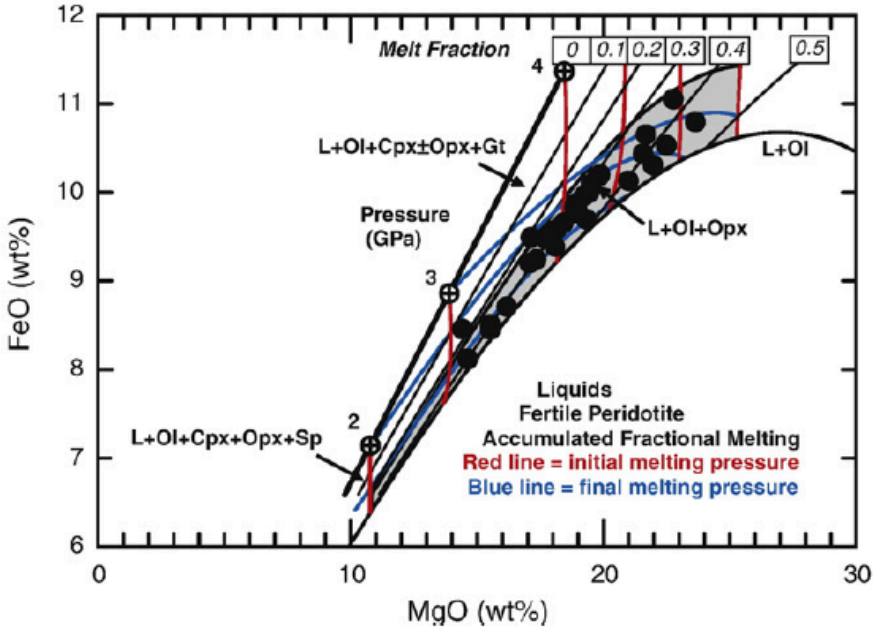

Fig. 3. MgO and FeO contents of model primary magmas for non-arc lavas of Archean and Proterozoic age compared with those of fertile peridotite. Black closed circles are primary magma solutions, from Table A1 in the Appendix. Black, blue and red lines are general solutions for melt fraction, pressure of final melting, and pressure of initial melting, respectively (Herzberg and O'Hara, 2002; Herzberg, 2004a; Herzberg and Asimow, 2008).

Herzberg&Gazel Nature 2009

Crystal/melt Fe partitioning

- Fe crystal chemistry: $^{2+}$Fe, $^{3+}$Fe
- $^{2+}$Fe: hexovalent in minerals, $^{3+}$Fe: tetravalent in minerals

Fayalite Fe_2SiO_4

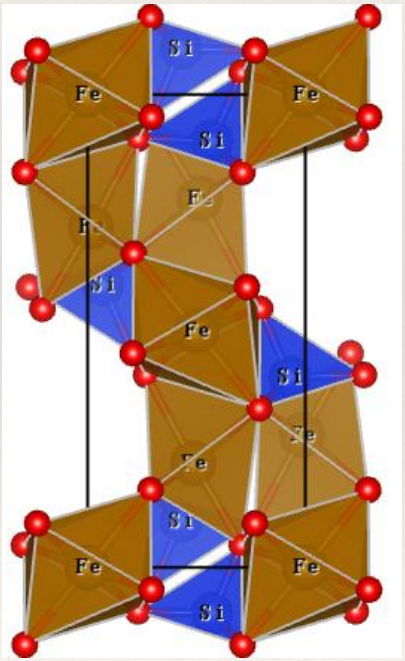

Hedenbergite $(Fe,Ca)_2Si_2O_6$

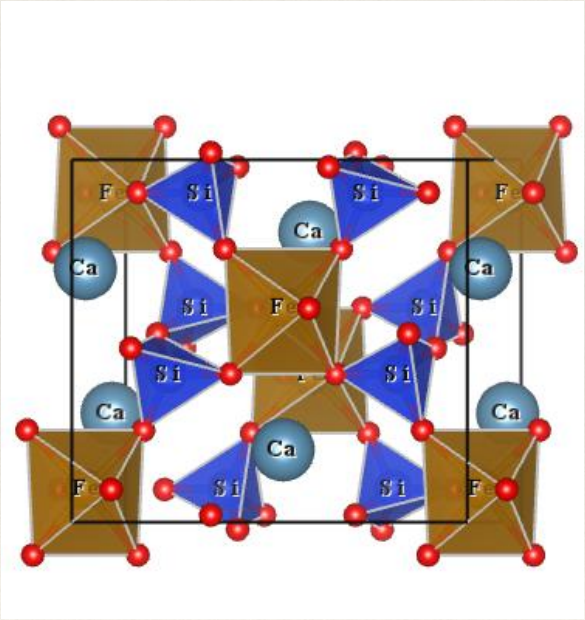

Crystal/melt Fe partitioning

- Fe crystal chemistry: $^{2+}$Fe, $^{3+}$Fe
- $^{2+}$Fe: hexovalent in minerals, $^{3+}$Fe: tetravalent in minerals
- $^{2+}$Fe: either IV or VI in melts (and possibly V)

Molten Fe_2SiO_4 | Molten $(Fe,Ca)SiO_3$ | Molten basalt

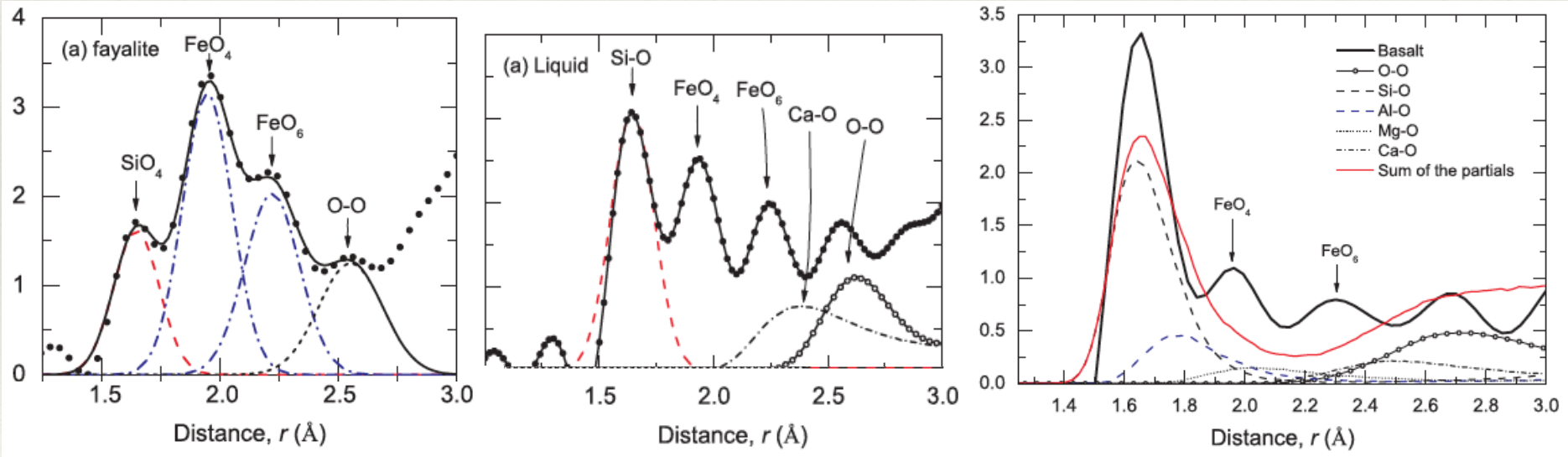

Drewitt et al. PRB 2013

Crystal/melt Fe partitioning

- Fe crystal chemistry: $^{2+}$Fe, $^{3+}$Fe
- $^{2+}$Fe: hexovalent in minerals
- $^{2+}$Fe: either IV or VI in melts (and possibly V)

XANES on glasses

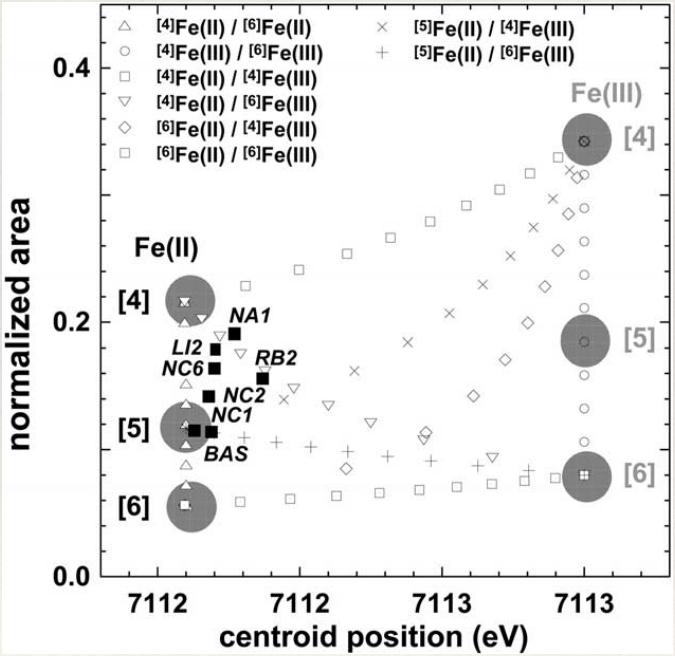

Jackson et al. GCA 2005

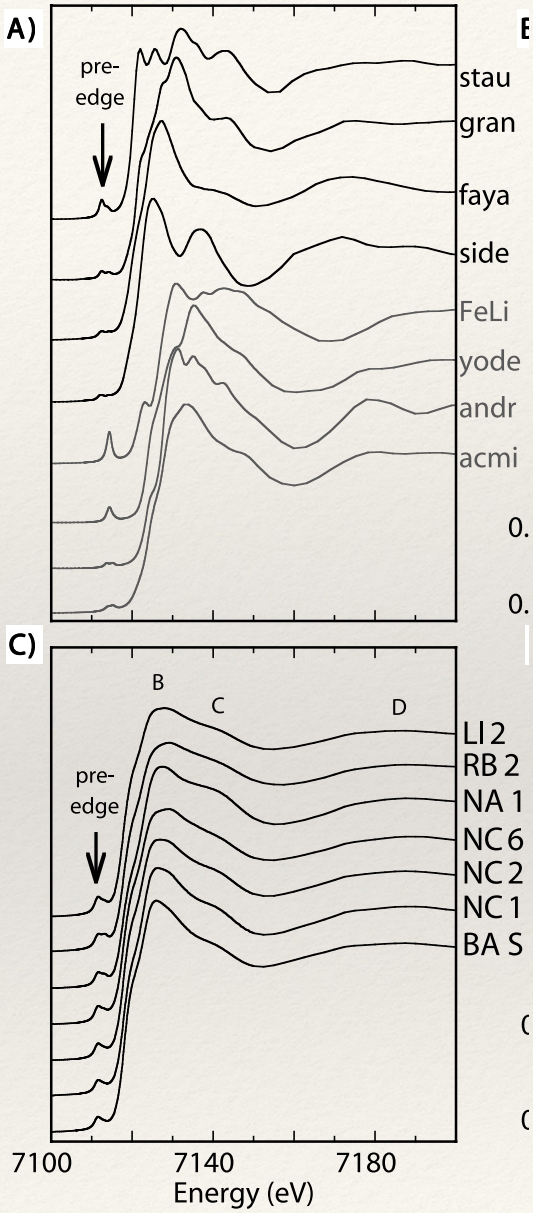

Crystal/melt Fe partitioning

- Fe bonding in crystals *vs* melts, consequences on isotope fractionation: basalts are enriched in heavy Fe isotopes

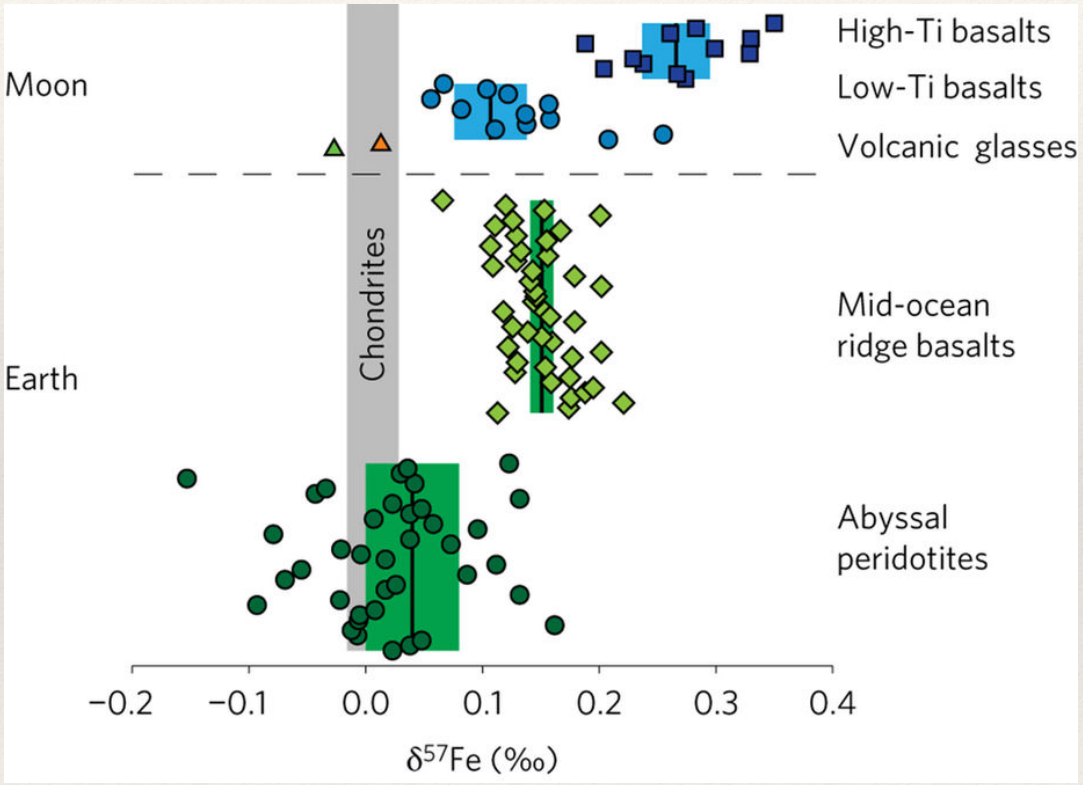

Elardo&Shahar Nat. Geo. 2017

Conclusions

- F. Albarède, Geochemistry (2009): "It remains a great challenge to predict the chemical properties of elements at very great depths"
- crystal-chemistry of element substitution well described
- melt 'crystal-chemistry' remains to be adequately modeled, matters at high pressure